Title
Leveraging Routine Surveillance to Measure, Map, and Monitor Malaria Burden in Uganda

Author
Epstein, Adrienne

Publication Date
2021

Peer reviewed|Thesis/dissertation

Leveraging Routine Surveillance to Measure, Map, and Monitor Malaria Burden in Uganda

by
Adrienne Epstein

DISSERTATION
Submitted in partial satisfaction of the requirements for degree of
DOCTOR OF PHILOSOPHY

in

Epidemiology and Translational Science

in the

GRADUATE DIVISION
of the
UNIVERSITY OF CALIFORNIA, SAN FRANCISCO

Approved:

DocuSigned by:
Bryan Greenhouse
3FD59F1CBAFD444...

Bryan Greenhouse
Chair

DocuSigned by:
Dr. Rodriguez-Barraquer
DocuSigned by:

Dr. Rodriguez-Barraquer

DocuSigned by:
Samir Bhatt
285BFBE1C971424...

Samir Bhatt

Committee Members

Contributions

A version of Chapter 1 in this dissertation was published in Malaria Journal on December 2, 2020. The Dissertation Committee Members supervised the research that forms the basis of this dissertation chapter. The published material is substantially the product of Adrienne Epstein's period of study at the University of California, San Francisco and was primary conducted and written by her. The work she completed for this published manuscript is comparable to a standard dissertation chapter.

Leveraging Routine Surveillance to Measure, Map, and Monitor Malaria Burden in Uganda

Adrienne Epstein

Abstract

Malaria is one of the leading causes of morbidity and mortality in sub-Saharan Africa, causing over 200 million cases and 405,000 deaths in 2017 (1). The World Health Organization states that quality malaria surveillance is essential to target regions and populations at highest risk, accurately measure changes in disease burden, and evaluate the impact of interventions (2). Surveillance data can also be used to produce meaningful indicators of malaria burden in order to identify determinants of disease and produce high resolution maps of risk (3, 4). This is essential because malaria transmission is heterogenous across space and time (5). Despite the critical need for high quality data, malaria surveillance is particularly poor in high burden countries (1).

The ideal indicator for estimating malaria morbidity in high transmission areas is case incidence, which is defined as the number of cases of malaria per unit time divided by the population at risk (3, 6, 7). The approach currently employed by most countries in sub-Saharan Africa to estimate malaria incidence involves cartographic methods that link parasite prevalence to incidence rates (8, 9). This method has several weaknesses. It relies on cross-sectional surveys that are costly, time-consuming, and infrequently performed. In addition, its accuracy is limited because the relationship between prevalence and incidence is variable and non-linear, particularly in high transmission settings. An alternative method of estimating incidence that is more direct, inexpensive, and comprehensive is the use of data reported through routine health management information systems (HMIS). Unfortunately, this is challenging because HMIS data are typically

not available at an individual patient level and lack information on where patients come from. Cases of malaria detected by the HMIS often lack laboratory confirmation. Furthermore, quantifying the denominator for incidence using these data is ambiguous because catchment areas around health facilities are not well defined.

The overall goals of this dissertation are to leverage surveillance data routinely collected at public health facilities in Uganda to improve measurement of malaria burden and to accurately capture changes in malaria burden across space and time. This dissertation is organized into three chapters. The first chapter used enhanced HMIS data to estimate care-seeking populations around health facilities and, with these estimates, to generate measures of malaria incidence over time. These estimates were then compared to "gold standard" measures of incidence measured concurrently in cohorts. Through developing this new method to generate catchment area populations, we found that our estimates of incidence accurately captured gold standard incidence and its dynamics over time. The second chapter aimed to map malaria incidence across Uganda using this new measure of incidence captured through enhanced HMIS data. Using spatio-temporal modeling, we generated predictions of malaria incidence in 2019-2020 at the parish-level in Uganda. The model performed well, particularly in areas where sentinel surveillance sites were more densely located across space. The findings from this analysis suggest that routinely collected health facility data could be used for risk mapping purposes. The third chapter used enhanced HMIS data to evaluate the impact of indoor residual spraying (IRS) in Uganda. We used data from 5 districts that received over 7 years of sustained IRS and compared monthly malaria burden to a baseline pre-IRS period. Our findings suggest that malaria burden declined 85% in the 4th and 5th year of sustained IRS, but increased in the 6th and

7th years. The timing of the increase in burden coincided with a switch in IRS active ingredient to a new chemical, clothianidin. These findings are an important call for more research aimed at studying the real world effectiveness of IRS with clothianidin.

Taken together, these chapters underscore the potential for routinely collected health facility surveillance data to answer important scientific questions and to inform policy.

Table of Contents

List of Figures

List of Tables

List of Abbreviations

aEIR: annual entomological inoculation rate

AIC: Akaike's information criterion

aIRR: adjusted incident rate ratio

CI: confidence interval

EVI: enhanced vegetation index

GAM: generalized additive model

GMRF: Gaussian Markov random field

HMIS: health management information system

IQR: interquartile range

IRR: incidence rate ratio

IRS: indoor residual spraying

LLIN: long-lasting insecticide treated nets

MAP: Malaria Atlas Project

MRC: Malaria Reference Center

NMCP: National Malaria Control Program

PPY: per person-year

RDT: rapid diagnostic test

TPR: test positivity rate

UMSP: Uganda Malaria Surveillance Program

VIF: variance inflation factor

WHO: World Health Organization

Chapter 1: Estimating malaria incidence from routine health facility-based surveillance data in Uganda

Adrienne Epstein, Jane Frances Namuganga, Emmanuel Victor Kamya, Joaniter I. Nankabirwa, Samir Bhatt, Isabel Rodriguez-Barraquer, Sarah G. Staedke, Moses R. Kamya, Grant Dorsey, Bryan Greenhouse

Abstract

Background

Accurate measures of malaria incidence are essential to track progress and target high-risk populations. While health management information system (HMIS) data provide counts of malaria cases, quantifying the denominator for incidence using these data is challenging because catchment areas and care-seeking behaviours are not well defined. This study's aim was to estimate malaria incidence using HMIS data by adjusting the population denominator accounting for travel time to the health facility.

Methods

Outpatient data from two public health facilities in Uganda (Kihihi and Nagongera) over a 3-year period (2011-2014) were used to model the relationship between travel time from patient village of residence (available for each individual) to the facility and the relative probability of attendance using Poisson generalized additive models. Outputs from the model were used to generate a weighted population denominator for each health facility and estimate malaria incidence. Among children aged 6 months to 11 years, monthly HMIS-derived incidence estimates, with and without population denominators weighted by probability of attendance,

were compared with gold standard measures of malaria incidence measured in prospective cohorts.

Results

A total of 48,898 outpatient visits were recorded across the two sites over the study period. HMIS incidence correlated with cohort incidence over time at both study sites (correlation in Kihihi=0.64, p <0.001; correlation in Nagongera=0.34, p=0.045). HMIS incidence measures with denominators unweighted by probability of attendance underestimated cohort incidence aggregated over the 3 years in Kihihi (0.5 cases per person-year (PPY) *vs* 1.7 cases PPY) and Nagongera (0.3 cases PPY *vs* 3.0 cases PPY). HMIS incidence measures with denominators weighted by probability of attendance were closer to cohort incidence, but remained underestimates (1.1 cases PPY in Kihihi and 1.4 cases PPY in Nagongera).

Conclusions

Although malaria incidence measured using HMIS underestimated incidence measured in cohorts, even when adjusting for probability of attendance, HMIS surveillance data are a promising and scalable source for tracking relative changes in malaria incidence over time, particularly when the population denominator can be estimated by incorporating information on village of residence.

Introduction

Malaria surveillance is widely recognized as an essential intervention to target regions and populations at high risk, accurately measure changes in disease burden, and evaluate the impact of interventions [1]. In many high burden settings, surveillance is conducted through passive case detection at health facilities as part of the routine health management information system (HMIS). There are several strengths in conducting HMIS-based surveillance: data provide direct measures of morbidity, are collected continuously over time, and cover a broad geographic range (10). However, these data are often hindered by reporting delays and gaps, poor data quality, health seeking behavior, and lack of laboratory-confirmed diagnostics (11, 12). For this reason, measures of malaria morbidity assessed with HMIS data tend to largely underestimate true burden (1, 11, 13-15).

An additional challenge with the utility of HMIS surveillance data is in translating case counts into meaningful metrics of malaria burden. A common HMIS-derived metric is the test positivity rate (TPR), defined as the proportion of individuals who test positive for malaria per 100 individuals tested. The TPR has several inherent limitations: it is prone to bias due to the incidence of non-malarial illnesses, has a non-linear relationship with malaria incidence, and cannot be translated into absolute estimates of incidence (7, 16-18). The most useful metric of malaria morbidity is malaria incidence, defined as the number of cases of malaria per unit time divided by the size of the population at risk (3, 7). The major challenge of translating HMIS data into accurate measures of malaria incidence is quantifying the denominator, because catchment areas around health facilities are not well defined. Previous efforts to quantify this denominator have relied on representative cross-sectional surveys with information on household care-seeking

(19, 20), an additional source of information that is costly to collect and requires population-level representativeness.

The aim of this study was to estimate malaria incidence over time, without the need for independent survey data on care seeking, using enhanced HMIS data. This study leveraged high quality, individual-level HMIS surveillance data, including information on village of residence for patients presenting to two Uganda Malaria Surveillance Programme (UMSP) Malaria Reference Centres (MRCs) over 3 years from 2011 to 2014. The relationship between travel time and outpatient attendance was modelled to generate a weighted population denominator for each MRC and estimate incidence over time. HMIS-derived incidence estimates where then compared to gold standard measures of malaria incidence measured prospectively in cohort studies conducted in sub-counties surrounding MRCs.

Methods

Study sites

This analysis used data from health facility-based malaria surveillance systems in two Ugandan sub-counties: Kihihi sub-county, Kanungu district and Nagongera sub-county, Tororo district. Both sub-counties are rural; at the time of the study, Kihihi exhibited moderate transmission intensity (annual entomological inoculation rate [aEIR] 2011-2013 = 32.0) and Nagongera high transmission intensity (aEIR = 310) (21). Both regions experienced two annual peaks in malaria burden following the rainy seasons.

From 2012-2014, the government of Uganda carried out a universal distribution of free long-lasting insecticide-treated nets (LLINs) with the goal of achieving one net per two people in each household. Nagongera sub-county received nets in November 2013 and Kihihi sub-county received nets in June 2014.

Health facility-based data

Enhanced malaria surveillance was established via the Uganda Malaria Surveillance Program (UMSP) MRCs in 2006, as previously described (22). UMSP conducts sentinel surveillance in 70 level III and IV public outpatient facilities in Uganda, including Kihihi Health Centre IV and Nagongera Health Centre IV. At each MRC, individual-level outpatient department records are entered into an electronic MS Access (Microsoft Corporation, Redmond, WA) database for all individuals presenting to the outpatient departments of the health facilities using a standardized format. Data collected includes patient demographics (age, gender, and village of residence), results of laboratory tests (rapid diagnostic test or microscopy), diagnoses given, and treatments prescribed. UMSP provides laboratory support and quality control training to ensure high quality diagnostic testing. Data are sent to the UMSP data centre and cleaned before transfer to Stata (Stata Corp, College Station, TX) for analysis. This analysis uses 3 years of health-facility based surveillance data from the two MRCs (September 2011-August 2014). These months were selected given the low level of missingness (<30%) for village of residence. This analysis was restricted to patients aged 6 months through 10 years to make them comparable to cohort data described below.

Cohort data

Dynamic cohort studies were conducted in children aged 6 months through 10 years from 100 households randomly selected from the two study sub-counties, as previously reported (21). In summary, eligible children from selected households were followed from August 2011 through June 2017. At enrollment, parents/guardians provided written informed consent and received an LLIN. Cohort participants received free medical care at designated study clinics located at the same MRCs where UMSP data were being collected; parents/guardians were encouraged to bring their children to the clinic any time they were ill. Children who presented with a fever (tympanic temperature ≥ 38.0°C) or history of fever in the previous 24 hours had a thick blood smear performed. If the blood smear was positive by microscopy, the child was diagnosed with malaria and provided treatment. Episodes of uncomplicated malaria were treated with artemether-lumefantrine; complicated or recurrent malaria occurring within 14 days of prior therapy was treated with quinine.

Measures

Malaria Suspected. Health-facility based surveillance recorded all outpatients as "malaria suspected" or "malaria not suspected." Malaria suspected was defined as patients who a) underwent a laboratory test for malaria (microscopy or rapid diagnostic test); or b) were given a clinical diagnosis of malaria in the absence of laboratory testing. Any record that did not meet these criteria was considered "malaria not suspected."

Malaria Cases. At MRCs, malaria cases were defined as patients with laboratory-confirmed malaria diagnoses (by microscopy or rapid diagnostic test).

Gold Standard Incidence. Malaria incidence measured through dynamic cohorts was considered the gold standard. Incidence was defined as the number of new episodes of malaria divided by the total person time observed. New episodes of malaria were defined as any episode of malaria not preceeded by another episode in the prior 14 days. A secondary definition using a parasite threshold of 2000 parasites/μL was also applied as a sensitivity analysis.

Statistical analysis

Travel Time Estimation. Villages located within Kihihi and Nagongera sub-counties were mapped during cross-sectional enumeration surveys conducted in 2009-2010 (21). These village shapefiles were linked to unique identifiers of villages found in the UMSP database. Villages of residence for all outpatients living within the MRC subcounty were identified and mapped.

Travel times were calculated using Malaria Atlas Project's friction surface 2015 raster file obtained through Google Earth Engine, available at 1-kilometer resolution (23). The authors of this friction surface combined datasets on roads, railways, water bodies, slope and elevation, landcover, and borders to calculate a nominal overall speed of travel across each pixel, in units of minutes of travel time per metre. Travel times represent Uganda-specific mean travel times associated with the road types in the pixel, or, in pixels where no roads are present, walking times. The malariaAtlas R package was used to calculate the mean travel time from each outpatient's village to the MRC of interest, in addition to the travel times to all nearest level III and IV health facilities (24). Travel times were defined as the minimum travel time between two points.

Care-seeking model. Observations were restricted to those residing in villages whose nearest level III or IV health facility was the MRC of interest, assuming that individuals attend their nearest health facility. These villages were defined as the MRC's "catchment area" (19). Since not all individuals seek care when ill, and this care-seeking behavior is driven in part by distance to the health facility, this analysis sought to account for this distance-specific care-seeking rather than using the raw population of the catchment area as a denominator for incidence. The probability of seeking care at the MRC was expected to decay as function of travel time to the facility. Relative village-level care-seeking probabilities were modelled and estimated as a function of travel time to the facility from each village within the catchment area. These probabilities were then used to down-weight village populations when estimating incidence. For example, if care-seeking from a particular village was estimated to be 80%, the population seeking care from that village was estimated to be 80% of the total population.

The care-seeking model was restricted to outpatients for whom malaria was not suspected. This group was used because their probability of attendance should be minimally biased by heterogeneity in malaria incidence across villages. Because this population represents a range of diagnoses, spatial bias is expected to be minimal. By using this population to model care-seeking, this analysis assumed that differences in care-seeking for outpatients not suspected of having malaria over space was driven solely by travel time to the health facility.

For each MRC, non-linear Poisson generalized additive models (GAMs) were specified to estimate the relationship between mean travel time from village *i* to the MRC and the count of

outpatients not suspected of having malaria who visited the MRC from village *i* from September 2011-2014. GAMs are a class of generalized linear models that allow for the relationship between the outcome and predictor to be estimated using smooth functions of the predictor variables (25). A non-parametric smooth function was applied to the travel time predictor, as the relationship between travel time to the facility and attendance was hypothesized to be non-linear. An offset for the logged population from village *i* derived from the High Resolution Settlement Layer (26) was included. To calculate relative village-level probabilities of attendance, predicted counts were estimated using the model described above holding the village population size constant. These counts were rescaled to relative probabilities by dividing the predictions by the predicted count in the village where the MRC is located. Calculating the relative probabilities in this way assumes that individuals living in the same village as the MRC have a probability of seeking care of 1.

In order to evaluate the sensitivity of these findings to the aforementioned assumptions, models were re-specified restricting outpatients to the top 5 diagnoses (including malaria) to determine whether the relationship between travel time and attendance differed across indications. In addition, stratified analyses were performed based on age category (6 months to < 5 years, 5 years to < 11 years) and gender. Models were also specified using straight-line distance from the centroid of the village of residence to the MRC as predictor and compared to results using travel time as predictor.

Incidence Estimation. HMIS data were used to estimate malaria incidence in two ways. First, incidence was estimated by dividing malaria cases over the catchment area denominator

(including all villages for which the MRC is the closest health facility) without down-weighting for travel time, hereafter called unweighted catchment incidence. Second, malaria incidence was estimated by dividing malaria cases by a weighted denominator using the weights described above to adjust village-level populations, hereafter called weighted catchment incidence. All populations were set to grow at a fixed rate each month based on the World Bank's estimate of population growth during the study window (0.29% monthly) (27). Both of these HMIS-derived measures were compared to metrics of gold standard (cohort) incidence by generating plots over time, calculating measures of pair-wise correlation by month, and comparing aggregated estimates of malaria incidence over the three year study window. This method assumes that relative treatment-seeking behaviour for non-malarial illness is the same as for malaria.

Results

Of the 118 villages mapped in Kihihi sub-county, 30 villages were included in the catchment area, totaling a population of 15,155 (**Figure 1.1**). Mean village-level travel times to the MRC ranged from 0 minutes to 40 minutes (mean 13 minutes). In Nagongera sub-county, 30 of 45 villages were included in the catchment area, totaling a population of 32,226. Travel times to the MRC ranged from 1 to 21 minutes (mean 10 minutes).

Health facility-based surveillance involved a total of 48,898 visits among children aged 6 months to 11 years over the 3-year observation period (**Table 1.1**). A total of 46.1% and 49.7% of these visits occurred among patients residing within the catchment areas of Kihihi and Nagongera, respectively. The proportion of outpatient visits from within the catchment areas suspected of having malaria was 88.9% and 88.7% in the two sub-counties, and over 98% of these individuals

underwent laboratory testing. The TPR within the catchment area was 50.0% in Kihihi and 43.8% in Nagongera. For the cohort studies, a total of 686 children were observed over 1,628 person-years over the 3-year observation period. A total of 3,778 episodes of malaria were diagnosed, with an average malaria incidence of 1.7 and 3.0 cases per person-year (PPY) at risk in Kihihi and Nagongera, respectively.

The relationship between travel time and the predicted probability of attendance is presented in **Figure 1.2**, and as expected decreased with increasing travel time in both sites. In Kihihi, the probability of attendance dropped steadily, plateaued at approximately 10 minutes, then continued to drop, with a slight increase at the furthest village included in the catchment area. In Nagongera, the probability of attendance dropped steadily until approximately 10 minutes travel time, then flattened at close to 10%. The shape of these curves was substantively similar to curves resulting from models using straight-line distance as predictor (**Appendix Figure 1.1**). The relationship between travel time and attendance was consistent across age groups and sexes (**Appendix Figure 1.2** and **Appendix Figure 1.3**). In Nagongera, these relationships were also consistent when stratifying by diagnosis. However, in Kihihi, the relationship between travel time and probability of attendance differed among those diagnosed with malaria, cough or cold, diarrhoea, and GI disorders, with a lower probability of attendance in the village where the health facility was located compared to villages with travel times around 10 minutes (**Appendix Figure 1.4**). Of note, the village where the MRC is located in Kihihi is urban and has a documented lower level of malaria transmission than surrounding villages (28).

The three incidence measures (weighted catchment incidence, unweighted catchment incidence, and cohort incidence) are plotted over time by age group in **Figure 1.3**. In most months across age groups and sites, both the weighted and unweighted catchment measures followed the same trajectory of cohort incidence. Weighted catchment incidence underestimated cohort incidence (with the exception of the first several months of observation in Kihihi), but less so than the unweighted measure. In Nagongera, weighted catchment incidence followed cohort incidence until the community-level LLIN distribution, when they diverged. When a parasite density of 2000 parasites/μL was applied to incident cohort cases the results were similar, but cohort incidence fell closer to weighted catchment incidence (**Appendix Figure 1.5**). The pairwise correlation between cohort and catchment incidence (both weighted and unweighted) was higher in Kihihi (corr = 0.64, $p < 0.001$) than Nagongera (corr = 0.34, $p = 0.045$). However, when restricting to the period of time prior to the universal LLIN distribution, the correlation in Nagongera was higher (corr = 0.72, $p < 0.001$).

Incidence estimates by age group and metric (cohort, weighted, and unweighted) aggregated over the 3-year observation period are presented in **Table 1.2**. These reflect the findings plotted in **Figure 1.3**, with the weighted incidence metric falling between cohort and unweighted incidence. To best understand bias in incidence estimates derived from enhanced HMIS data, weighted catchment incidence was compared to cohort incidence for each month, stratified by age (**Figure 1.4**). In Kihihi, health facility-based incidence initially overestimated cohort incidence (approximately 2-fold or 1 episode of malaria PPY), then underestimated incidence (approximately 50% or 2 episodes of malaria PPY, **Figure 1.4**). This trend in overestimation followed by underestimation was consistent across age groups. In Nagongera, weighted

catchment incidence consistently underestimated cohort incidence, particularly after community level LLIN distribution: during the final year of observation. Unlike Kihihi, different degrees of bias in estimation by age group were observed, with relative incidence in younger children consistently underestimated to a larger degree than older children. In absolute terms, however, the differences were very similar between age groups until after community level LLIN distribution where incidence was underestimated to a larger degree in older children.

Discussion

This study used routinely collected HMIS data to estimate malaria incidence longitudinally and validated these estimates by comparing them to gold standard measures in moderate and high burden settings. Findings suggest that temporal changes in HMIS-based measures correlated reasonably well with a gold standard measure of incidence over time. Weighted estimates, which leveraged information on village of residence and travel time to the health facility to account for differences in care-seeking behaviour, fell much closer to the gold standard incidence than unweighted estimates that incorrectly assumed all individuals in the assigned catchment areas had a uniform probability of attendance. However, even using weighted estimates, HMIS data produced estimates of malaria incidence that were consistently lower than estimates from cohort studies, suggesting that not all episodes of malaria were being captured through the HMIS system. Nevertheless, these findings contribute to a broader literature indicating that HMIS data, particularly when analysed accounting for care-seeking behaviour, have potential to provide a relatively inexpensive data source to estimate key metrics of malaria burden across space and over time (3, 21, 29).

Findings from this study indicate that as travel time to the facility increased, the probability of health facility attendance fell precipitously. This was especially true in Nagongera, where the probability of attendance decreased by 50% as the travel time increased by onlt 5 minutes. One potential explanation is that the friction surface's resolution was too crude (1 km x 1 km) for village-level estimates. However, the steepness of these curves were also found when straight-line distance was used as a predictor. Another possibility is that there may be private health facilities and pharmacies within the area competing for care-seeking; the location of these facilities were not considered when estimating the catchment area.

Estimating malaria incidence from HMIS data has surveillance and programmatic benefits. A common measure derived from HMIS data is the TPR, which is often used as a proxy measure for measuring temporal trends in malaria incidence (3) and assessing the impact of control interventions (30, 31). However, the TPR is not informative about absolute case counts and, therefore, cannot be used for planning purposes (for example, when determining counts of anti-malarial medications to send to facilities) nor for estimating cases averted by control interventions. This is because the TPR correlates poorly with malaria incidence, especially in particularly low and high transmission settings, and does not capture differences between facilities (17). Incidence, alternatively, is an absolute measure of burden in the population; using HMIS data to measure malaria incidence longitudinally, therefore, would allow trends in the absolute burden of disease to be tracked over time and across space.

There are several potential reasons why HMIS-based measures consistently underestimated cohort incidence even after down-weighting the population denominator. First, the assumption

that care-seeking is 100% in the village where the facility is located may be incorrect; if care-seeking is lower, true incidence is underestimated. Second, there are key differences between the populations that participated in the cohort studies and the broader population throughout the sub-county. The cohorts represented a unique situation where barriers to care-seeking were removed through travel reimbursement, minimal waiting time and no hidden costs; therefore, health facility attendance was essentially universal. The underestimation of the weighted HMIS measure may therefore be explained by differences in care-seeking behaviour other than travel time, such as financial and time burdens or care-seeking at different facilities, such as lower level public facilities or private facilities. In Nagongera, this underestimation was more pronounced in older age groups. This may be due to differential care-seeking behaviours for caregivers of older children; this phenomenon (lower rates of care-seeking among caregivers of older children compared to children under 5) has been previously reported in Ethiopia and Malawi (32, 33).

One potential reason is that older children have greater immunity to clinical malaria and therefore a higher threshold for seeking care. Another potential explanation is that older children in this high transmission setting commonly have asymptomatic parasitaemia. In the cohort setting, these children may be more likely to seek care if they had fever (for any reason) and, in the presence of asymptomatic parasitaemia, would be classified as clinical/symptomatic malaria. Thus, the cohort incidence may in fact overestimate incidence of malaria episodes in older children in high burden settings, which is consistent with the results from applying a parasite threshold of 2000 parasites/μL to the definition of cohort incidence. It is unclear why these findings – the observed differential underestimation of incidence by age – were not echoed in

Kihihi, though this could be related to the lower transmission in Kihihi compared with Nagongera.

There was a divergence of HMIS and cohort incidence following the 2013 universal LLIN distribution in Nagongera. The 2013 distribution was the first universal LLIN distribution in Uganda. Evidence suggests that LLIN ownership and use was quite low before the distribution; the 2011 Uganda Demographic and Health Survey found that only 27% of households had at least one LLIN per two people (34). Participants in the cohort were given LLINs upon enrollment and, therefore, may have already experienced the individual and household-level benefits of LLIN utilization on malaria incidence; this divergence may be due to the broader population receiving LLINs later in the observation period and the likelihood of community-level benefits of LLIN use. Previous work concluded that there was no significant change in malaria incidence among cohort participants following community-level LLIN distribution in Nagongera (35). These results suggest that the impact on community incidence may have been larger than previously indicated based on the cohort data alone.

This study contributes to the literature by proposing a novel method to more accurately estimate malaria incidence from HMIS data using improved estimates of the population denominator. Previous work to estimate care-seeking probabilities to apply to incidence denominators has relied on representative, cross-sectional surveys that ask individuals about their care-seeking behaviour (19, 20, 36-38). These surveys are costly and are not conducted regularly, and the questions are often non-specific in that they do not ask respondents which health facility they attended. This study instead leveraged continuously available outpatient information on

geographic location of residence, information that is part of the standard outpatient registers at Ugandan health facilities. Estimating catchments using this information has utility beyond measuring incidence of malaria, such as assessing access to care in low-resource, high-burden settings (39), and assessing seasonal changes in health-seeking behaviour. If not already collected, health facility systems should consider adding geographic information to their routine data collection. In countries where these data are collected, Ministries of Health may consider an investment in training and support for health workers to ensure data completeness and accuracy; in recent years, UMSP has emphasized data completeness for geographic variables and brought missingness down to below 5% across all 70 sites. These data could then be linked to geocoded information on administrative units, data which are increasingly publicly available, allowing for georeferenced information on patients' origins.

This study has several limitations. First, the gold standard used in this study – malaria incidence measured in cohorts of children 6 months to 11 years of age – may not represent the true malaria incidence in the underlying community. Care-seeking patterns in the cohorts were in the setting of a research study and may not reflect real world behaviors. Second, absolute care-seeking probabilities were not possible to estimate with these data. This is because cross-sectional survey data on care-seeking behaviours in the villages around the MRCs are not available. Thus, the estimates of the denominator for incidence represent an improved upper bound compared to estimates without weighting, and the estimates of malaria incidence represent an improved lower bound. The inability to generate absolute probabilities poses challenges with comparing incidence between health facilities because care-seeking behaviours may differ across sites. However, treatment for malaria is free in Uganda and there is some evidence that care-seeking is

quite high: the 2018-2019 Malaria Indicator Survey found that 87% of caregivers sought treatment for children with fever in the 2 weeks preceding the survey (40); this figure may be higher in villages that are closest to the health facility. Thus, the assumption that care-seeking is close to 100% in the village where the health facility is located may be plausible. Finally, the High Resolution Settlement Layer, which combines satellite, census, and Facebook data to generate high resolution population estimates (26) for the population denominator undoubtedly contain uncertainty.

Conclusions

This study underscores the potential for HMIS data to estimate key metrics of malaria burden. Although cases captured at the health facility will likely continue to underestimate true burden, health facility metrics with estimation of population denominators accounting for care seeking may still allow for measurements of changes in burden over time. In practice, estimating catchment area denominators using down-weighting may be best applied in sentinel surveillance sites across high burden countries, due to the required methodological and time investments. Alternatively, instead of using a model to estimate care-seeking, health systems could aim to measure where people reside and catchment areas could be defined including patients living immediately around the health facility where care-seeking can be assumed to be essentially universal, notably in Uganda where public health care is free. This would require a modest investment in time and training of health professionals to include geographic information in the collection of patient demographics. With this information, HMIS data can be used to generate quality measures of malaria incidence that are relatively inexpensive, an essential tool for countries around the globe as they aim to achieve targets towards control and elimination.

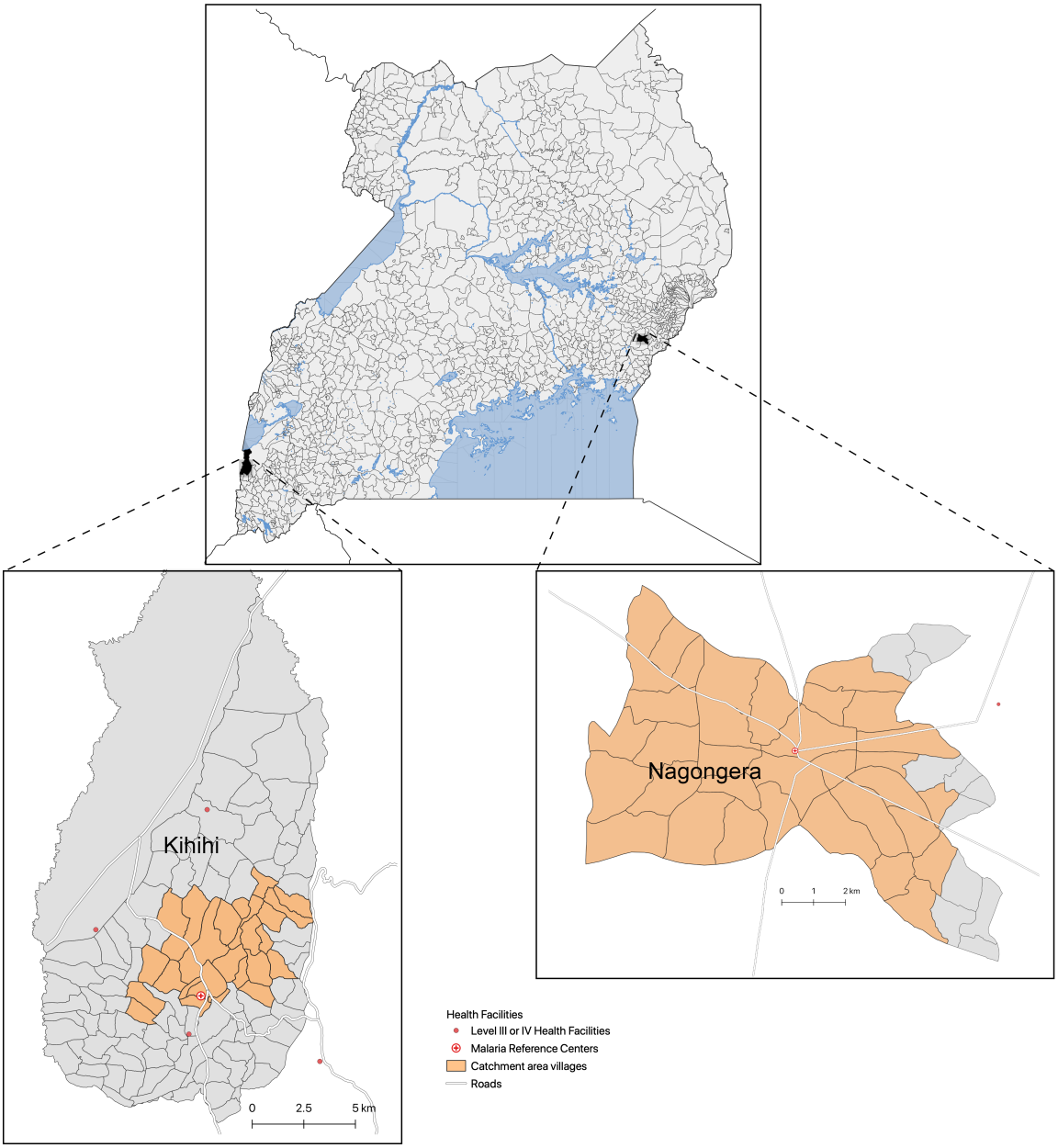

Figure 1.1. Map Malaria Reference Centers and their catchment areas in Kihihi and Nagongera sub-counties.

Table 1.1. Summary statistics from health facility-based and cohort surveillance studies; September 2011-August 2014			
Data Source	**Metric**	**Study Site**	
		Kihihi	**Nagongera**
Malaria Reference Centers	Outpatient visits for children aged 6 months - < 11 years	20,742	28,156
	Outpatient visits for children aged 6 months - < 11 years from catchment area (percent of total)	9,555 (46.1%)	13,985 (49.7%)
	Malaria suspected from catchment area (percent of total from catchment area)	8,497 (88.9%)	12,401 (88.7%)
	Diagnostic test performed (percent of malaria suspected from catchment area)	8,493 (99.9%)	12,238 (98.7%)
	Tested positive for malaria in catchment area (percent of tested from catchment area)	4,247 (50.0%)	5,358 (43.8%)
Cohort Studies	Number of children observed	353	333
	Person-years of observation	848	780
	Number of episodes of malaria	1,474	2,304
	Incidence of malaria (new episodes per person-year)	1.7	3.0

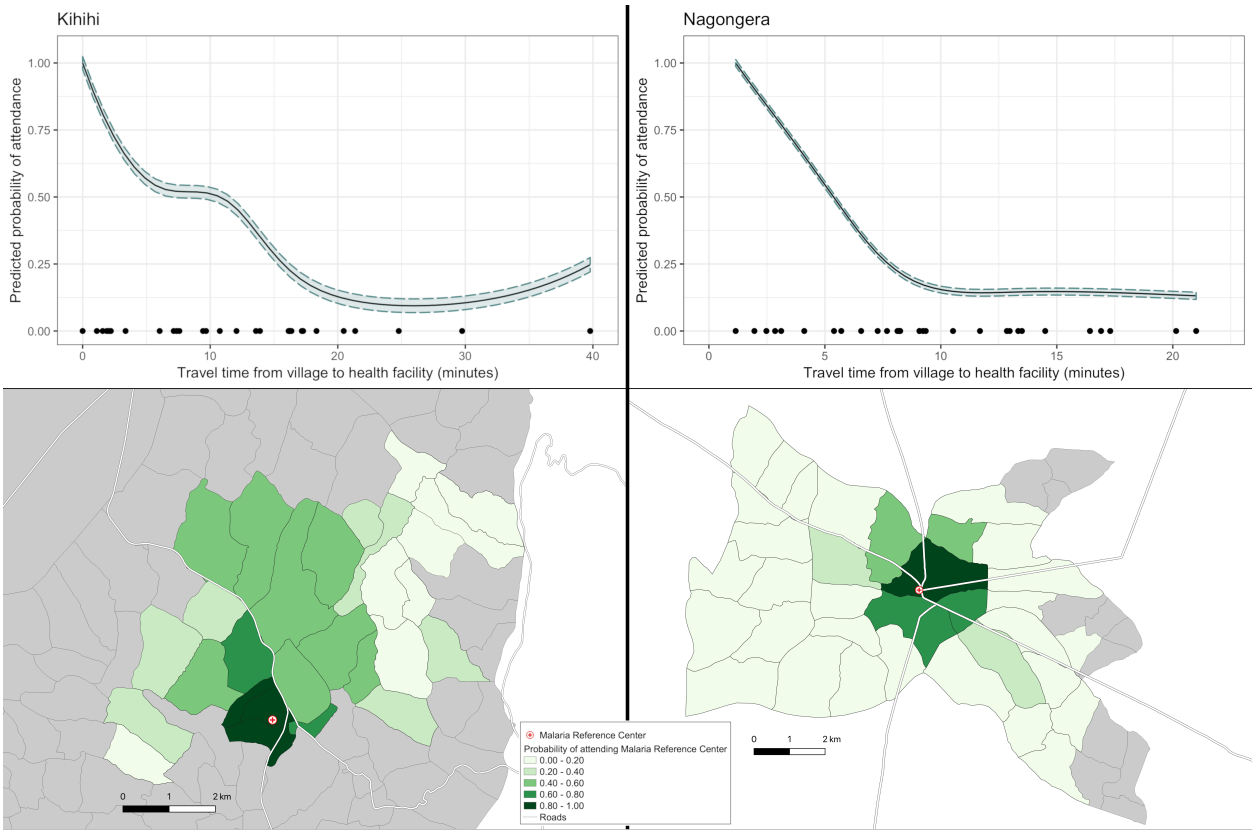

Figure 1.2. Modeled relationship between travel time to the health facility and probability of attending the health facility (top) and map of village-level probabilities of attendance (bottom).

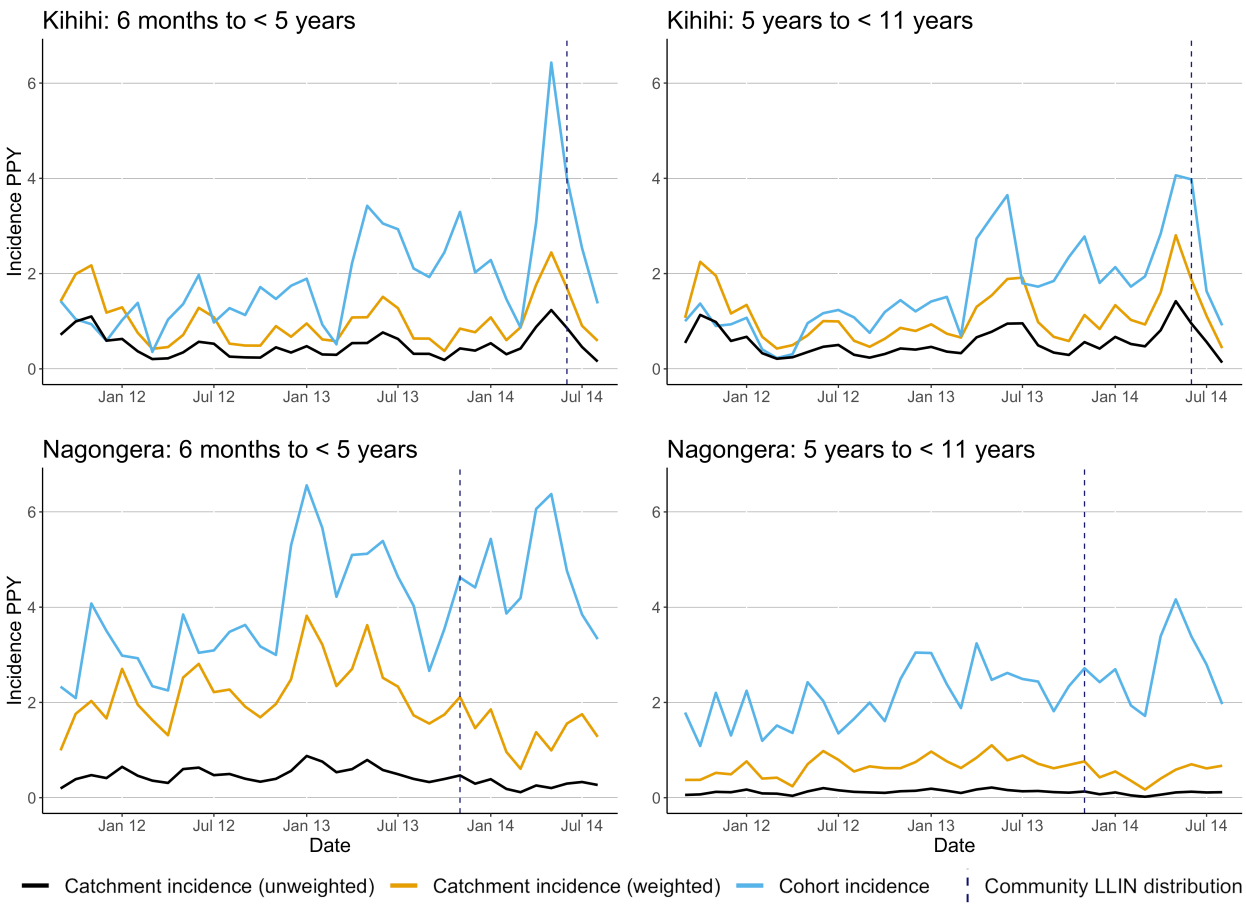

Figure 1.3. Incidence of malaria over the 3-year observation period measured in cohorts and using health facility-based surveillance.

Table 1.2. Malaria incidence PPY measured at surveillance sites from September 2011-August 2014.						
	Kihihi		**Nagongera**		**Nagongera (pre-November 2013 LLIN distribution)**	
	6 months to < 5 years	**5 years to < 11 years**	**6 months to < 5 years**	**5 years to < 11 years**	**6 months to < 5 years**	**5 years to < 11 years**
Cohort incidence	1.79	1.70	3.95	2.29	3.72	2.11
HMIS Weighted incidence	1.01	1.11	1.99	0.63	2.22	0.67
HMIS Unweighted incidence	0.50	0.55	0.43	0.12	0.50	0.13

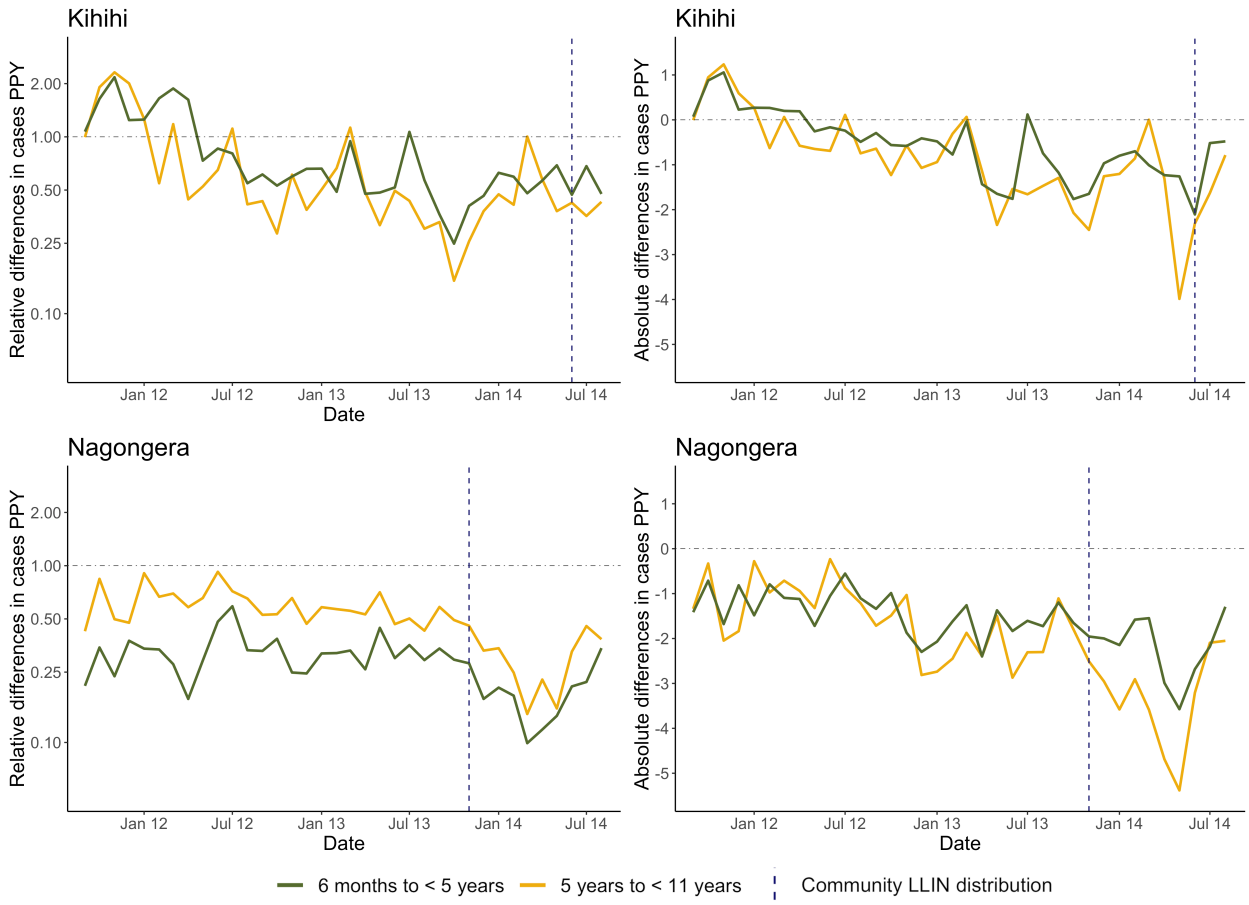

Figure 1.4. Absolute and relative differences between weighted and cohort incidence.

Chapter 1 Appendix

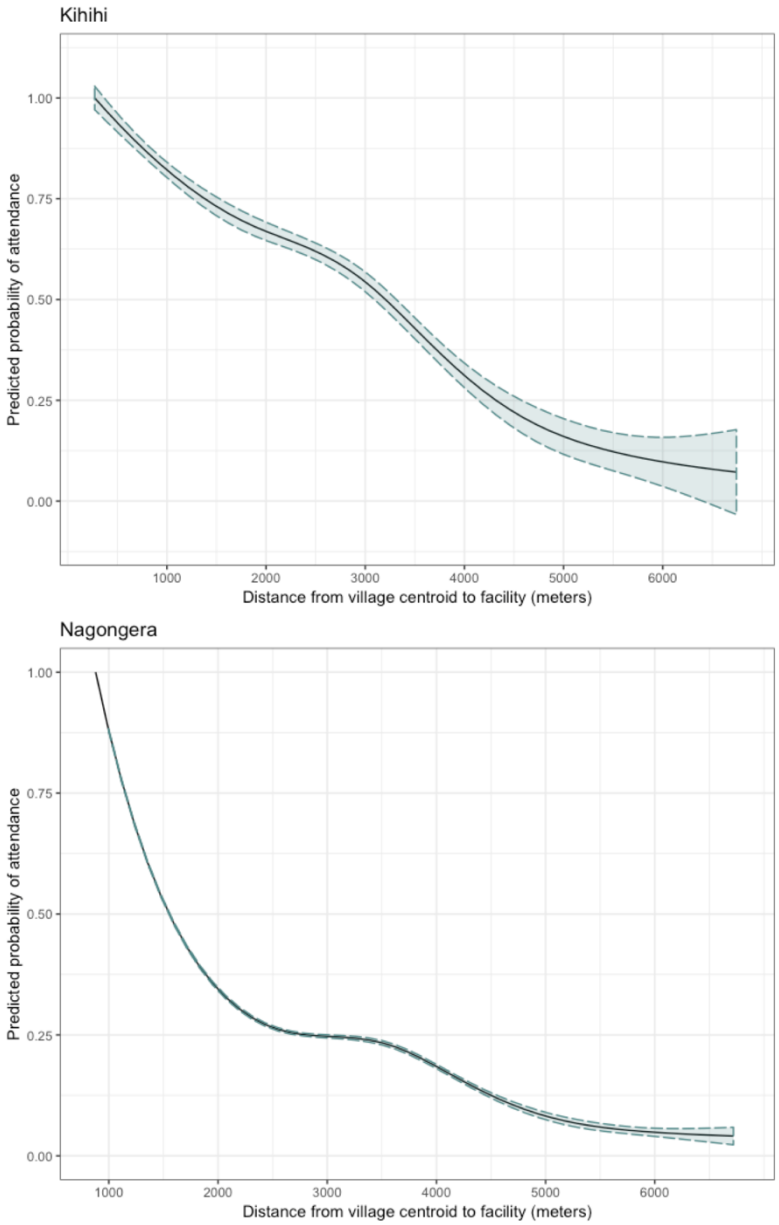

Appendix Figure 1.1. Modeled relationship between village centroid and the health facility and probability of attending the health facility.

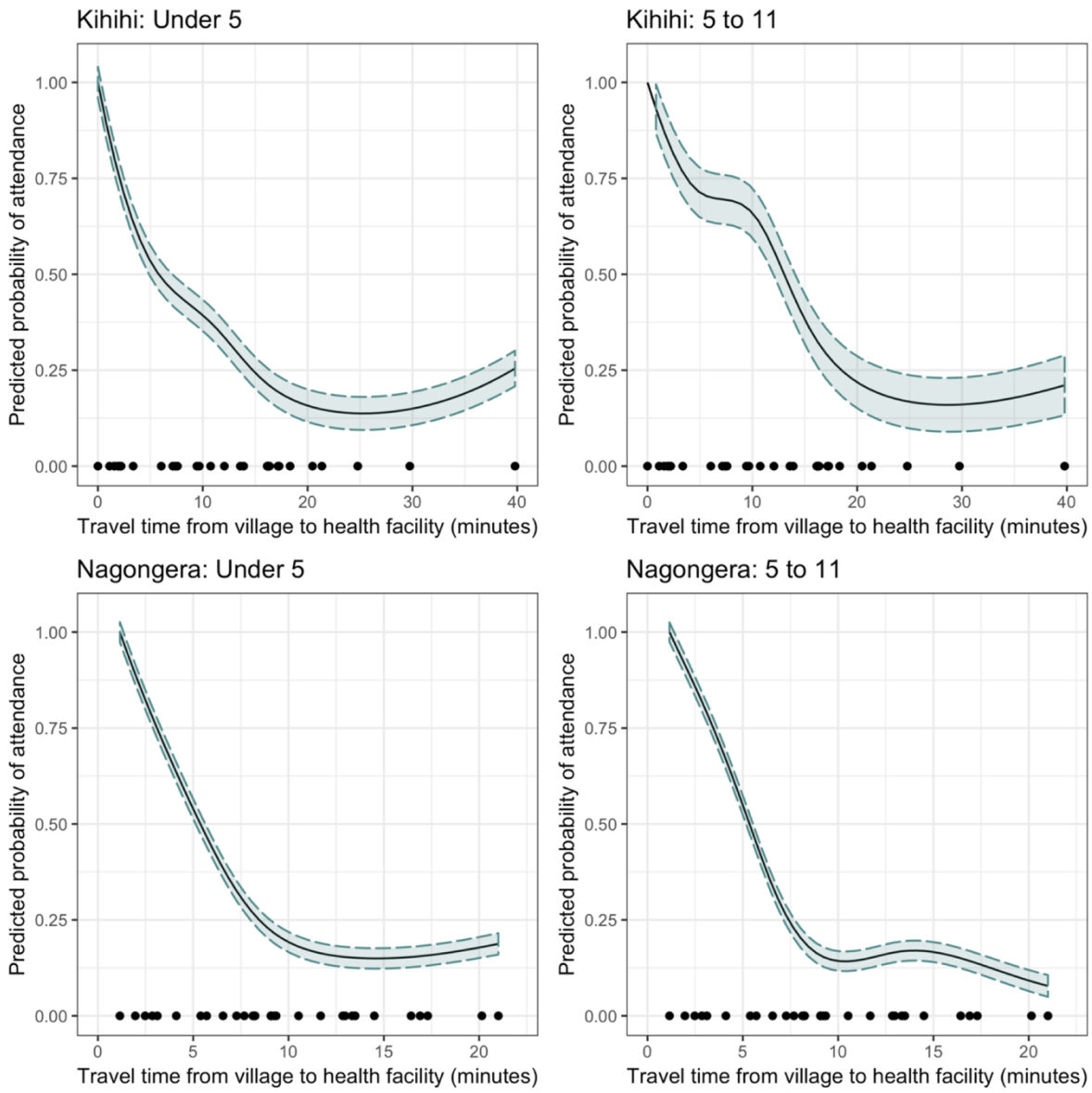

Appendix Figure 1.2. Predicted probabilities and 95% confidence intervals of attending the health facility among patients not suspected of having malaria stratified by age.

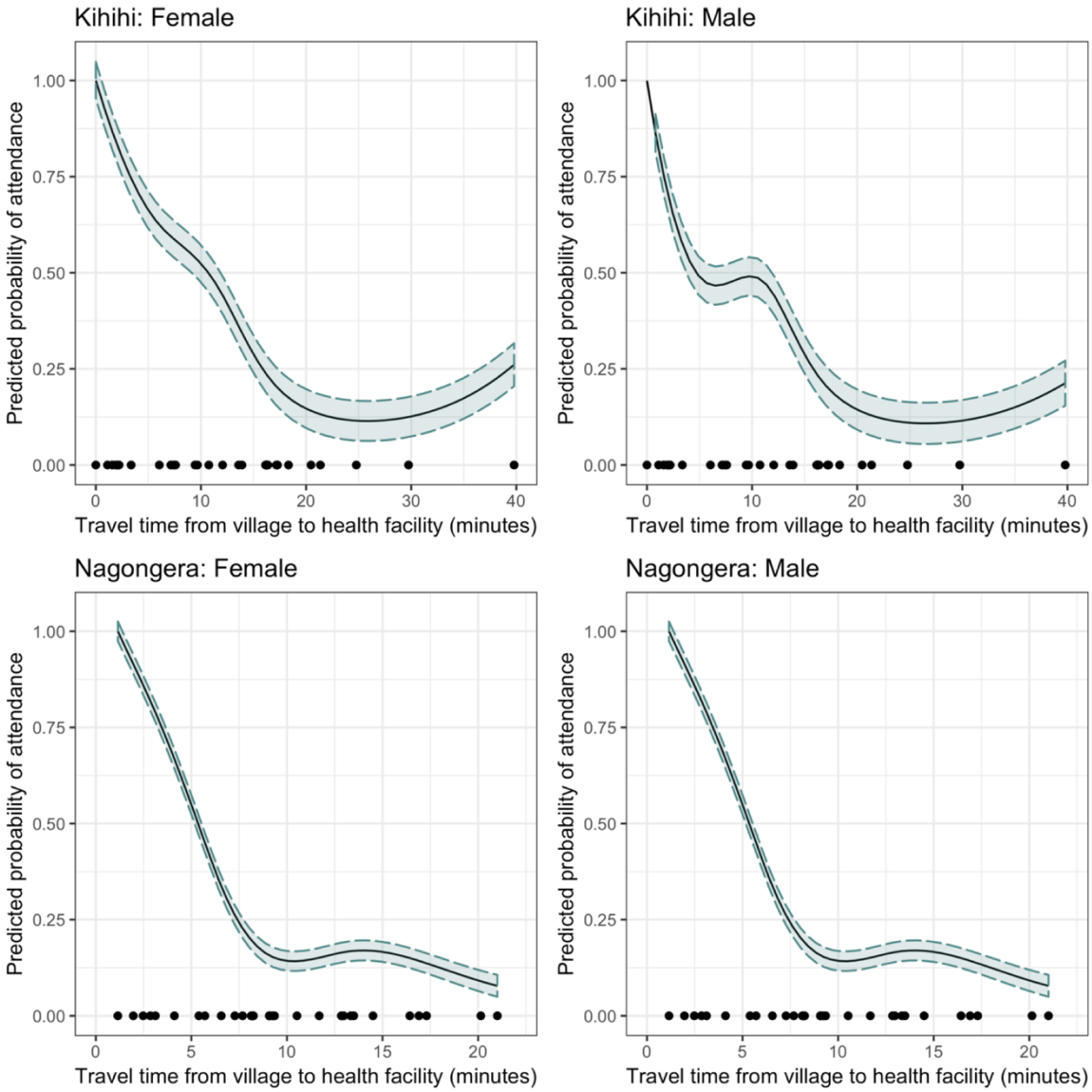

Appendix Figure 1.3. Predicted probabilities and 95% confidence intervals of attending the health facility among patients not suspected of having malaria stratified by sex.

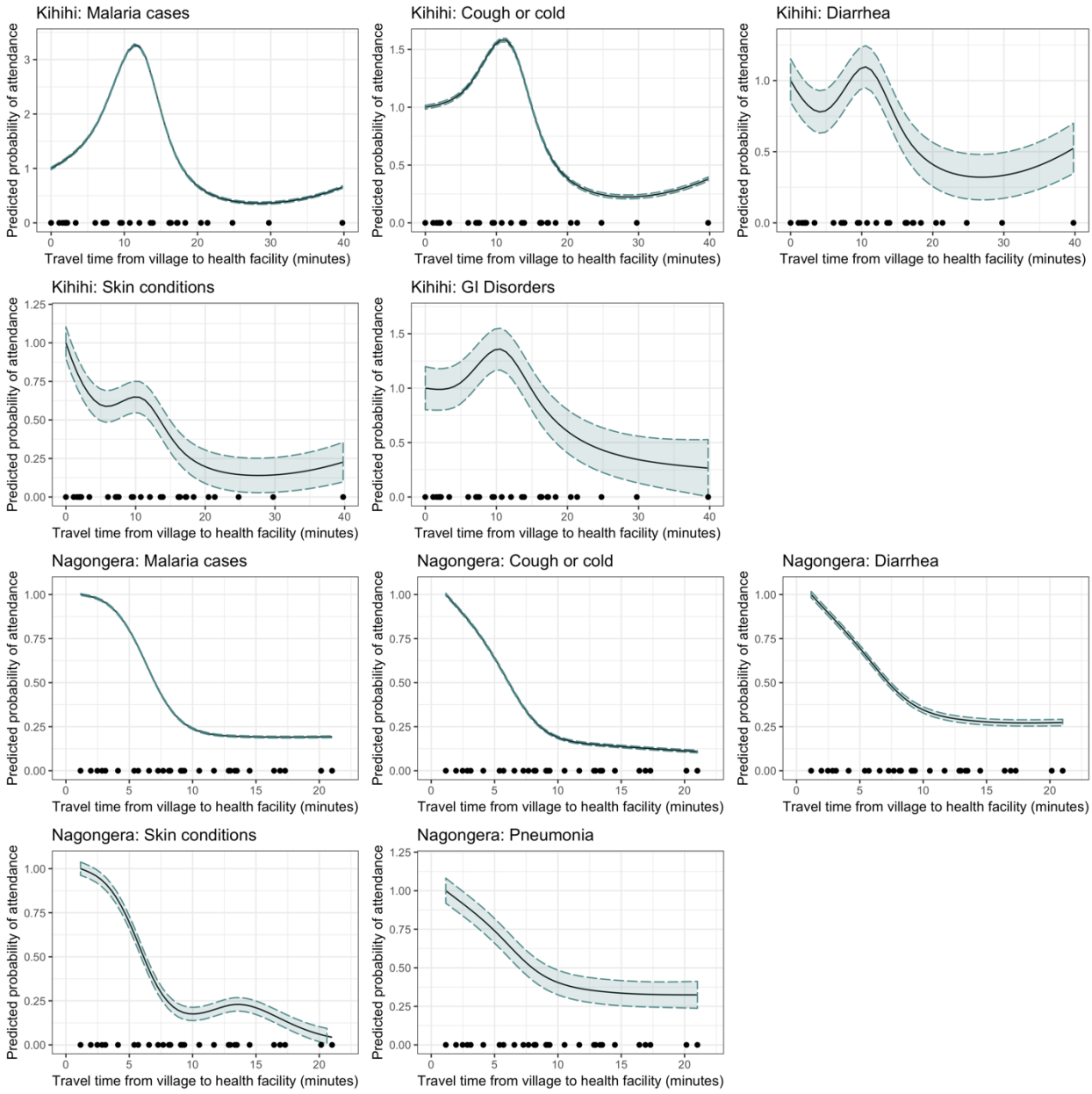

Appendix Figure 1.4. Predicted probabilities and 95% confidence intervals of attending the health facility among patients not suspected of having malaria stratified by the 5 most common diagnoses.

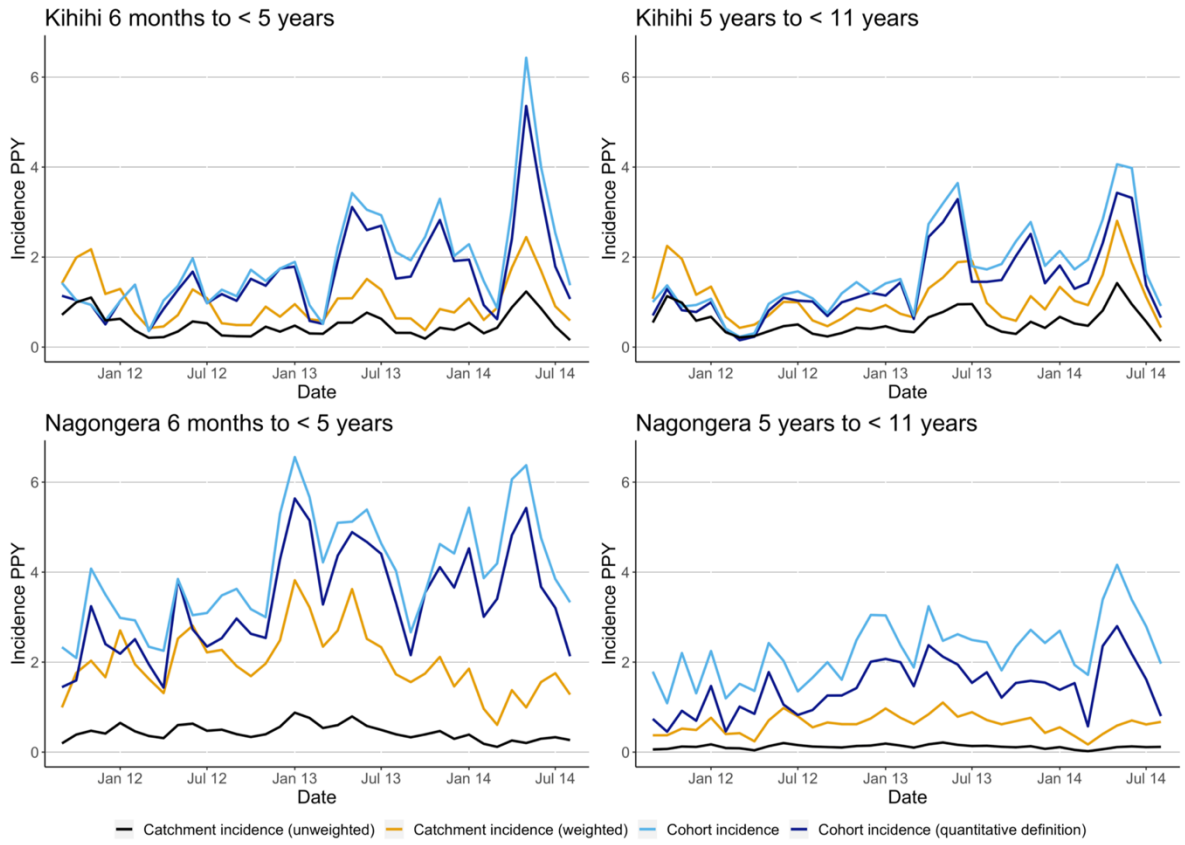

Appendix Figure 1.5. Incidence of malaria over the 3-year observation period measured in cohorts with additional parasite threshold definition and using health facility-based surveillance.

Chapter 2: Mapping malaria incidence using health facility surveillance data in Uganda

Adrienne Epstein, Jane Frances Namuganga, Isaiah Nabende, Emmanuel Victor Kamya, Moses R. Kamya, Grant Dorsey, Samir Bhatt, Isabel Rodriguez-Barraquer, Bryan Greenhouse

Abstract

Background

Maps of malaria risk are important tools for allocating resources and tracking progress. Most malaria risk mapping methods rely on cross-sectional surveys of parasite prevalence, but health facilities represent an underutilized and powerful source of data. This study's aim was to measure, model, and map malaria incidence in Uganda using outpatient data from 74 health facilities in 2019-2020.

Methods

Using 24 months of individual-level outpatient data routinely collected from 74 health facilities across Uganda (n=445,648 laboratory-confirmed cases), monthly measures of malaria incidence were estimated for parishes around health facilities (n=310). A spatio-temporal generalized additive model with spatial autocorrelation modeled using Gaussian Markov Random Fields was developed to generalize these estimates to the rest of Uganda. The model was informed by environmental, sociodemographic, and intervention variables over the 24-month study period. Estimated malaria incidence and its uncertainty were mapped at the parish level across Uganda (n=7,569) and compared to other metrics of malaria burden used by the Ugandan Ministry of Health.

Results

Over 4,659 parish-months of data, malaria incidence averaged 710 cases per 1,000 person-years (range 0 to 11,166), with substantial spatial and temporal variation. Maps resulting from spatio-temporal models indicated high burden in the north and northeast of Uganda, with substantially lower incidence in the 14 districts receiving indoor residual spraying. District-level estimated malaria cases correlated with cases reported by the health management information system (corr = 0.61, $p < 0.0001$), but was considerably higher (40,166,418 cases of malaria estimated across 24 months compared to 27,707,794 cases reported in the same period), indicating the potential for underreporting of malaria cases by the health management information system. Modeling of counterfactual scenarios suggest that approximately 5 million cases were averted due to indoor residual spraying of insecticide across the 24-month period.

Conclusions

Outpatient information routinely collected by health management information systems can be a highly valuable source of data for measuring and mapping malaria burden with minor modifications to enhance routine reporting, including reporting data at the individual level and utilizing information on patients' location of residence. National Malaria Control Programs may consider investing in robust surveillance systems embedded in public health facilities as a low-cost, high benefit tool to identify vulnerable regions and track the impact of control interventions.

Introduction

Understanding the spatial distribution of malaria burden is critical for identifying high transmission areas, evaluating local effectiveness of control efforts, and targeting future interventions to areas of greatest need (3, 41). However, most existing maps of malaria risk have inadequate operational utility for local decision making because they are low in resolution and rely on poor surveillance indicators such as parasite prevalence collected with limited geographic and temporal representativeness (19, 42-45). More advanced mapping techniques require an additional step of converting parasite prevalence to malaria incidence using mathematical modeling methods. While incidence is an improved indicator relative to parasite prevalence as it is a direct measure of burden, these models are difficult to reproduce, require advanced statistical skills, and rely on assumptions about the relationship between prevalence and incidence that may be wrong. Health management information system (HMIS) information collected routinely through the public health system represents an underutilized source of rich data that could be used for high-resolution risk maps of malaria incidence (15, 46). These data may have limitations including poor case ascertainment, inadequate reporting rates, reporting of only aggregate case data, and ambiguous population denominators around health facilities (19, 47, 48). However, they exhibit important strengths: they a provide direct measure of morbidity, are collected continuously over time, cover a broad geographic range, and are relatively inexpensive to collect (15, 46).

One country that could benefit from high resolution maps of malaria burden is Uganda. Malaria remains one of the leading health problems of Uganda despite rigorous efforts to improve vector control and case management over the past several decades (41, 49). The burden of malaria is

heterogeneous across the country; in some areas, burden is low due to geographic and climate variation and in others due to the successful deployment of vector control measures such as indoor residual spraying (IRS) (50, 51). High resolution maps of malaria risk could be utilized by the country's National Malaria Control Program (NMCP) to best target its resources: for example, at present, funding is only available to cover 14 of the 135 districts in the country with IRS. In addition, these maps could be used to evaluate the impact of interventions – a crucial step towards maximizing the limited resources available and allowing Uganda is to meet its targets established by the by the World Health Organization's Global Technical Strategy for malaria, including reducing malaria incidence from 2015 by at least 90% by 2030 (52).

In this analysis, we use enhanced health facility surveillance data to measure and map malaria incidence in Uganda in 2019-2020. First, we generated high resolution monthly estimates of malaria incidence at 74 health facility surveillance sites across the country by modeling catchment area populations around facilities. Second, we built a spatio-temporal prediction model for malaria incidence using sociodemographic, environmental, and intervention covariates. Third, we used this model to map malaria risk across Uganda and compare predicted estimates from our model to other measures used by the NMCP and to model counterfactual vector control intervention scenarios.

Methods

Enhanced Health Facility Data

The Uganda Malaria Surveillance Program (UMSP) has been conducting enhanced malaria surveillance in level III and IV public outpatient facilities in Uganda, called Malaria Reference

Centers (MRCs), since 2006 (22). At each MRC, individual-level data are entered into an electronic Microsoft Access database for all individuals presenting to the outpatient department using a standardized format. Information collected on outpatients includes demographics (sex, age, and village/parish of residence), results of laboratory tests (rapid diagnostic test or microscopy), diagnoses given, and treatments prescribed. UMSP provides laboratory support and quality control training to ensure high quality diagnostic testing, adherence to recommended case management, and data completeness. This analysis uses 2 years (24 months) of health-facility based surveillance data from 74 UMSP MRCs (**Figure 2.1**), from January 2019 through December 2020. This study window was selected to maximize the number of UMSP MRCs operating during the analytic period as 49 new UMSP sites were opened in 2019 and 2020. For information on the number of months each site contributed to the analysis, see **Appendix Table 2.1**.

Covariate Data

A set of environmental and socio-demographic variables known to be associated with malaria burden (53) were considered as candidate predictors for model selection (**Table 2.1**). Dynamic covariates including precipitation (54), daytime and nighttime land surface temperature (55), and enhanced vegetation index (EVI) (56), were aggregated to monthly measures. A series of lags (0, 1, 2 and 3 months prior to the month of outcome data) were considered in models, given the potential for delayed impacts of environmental variables and malaria outcomes. MODIS products (temperature and EVI) underwent gap-filling using a random forest model to adjust for gaps due to cloud cover (code available at https://github.com/disarm-platform/gapfilling_rasters).

Static covariates include elevation measured through the Shuttle Radar Topography Mission (57), slope (58), population density (59), distance to major roads and to major waterways (59), the prevalence of improved housing (60), and the presence of nighttime lights (61).

We also included district-level variables representing vector control interventions. These include a count of the number of months since the most recent long-lasting insecticide treated bednet (LLIN) distribution and a the number of months since the latest IRS campaign (by a binary indicator variable that takes the value of 1 if the site is in an IRS district or 0 of the site is in a non-IRS district).

Estimation of Malaria Incidence Outcome

To quantify malaria incidence at each MRC, catchment area population estimates were needed to serve as a denominator. To obtain these estimates, we modeled catchment area populations using a method previously described (62). In brief, we calculated village-level travel times to each MRC using Malaria Atlas Project's friction surface 2015 raster file (23). Using information on each outpatient's village of residence, we estimated a care-seeking model for the relationship between travel time and probability of attending the MRC using non-linear Poisson generalized additive models. This relationship was estimated among outpatients not suspected of having malaria because their probability of attendance is less likely to be directly correlated with malaria incidence across villages. This model implicitly assumed that differences in care-seeking for outpatients not suspected of having malaria over space was driven exclusively by travel time to the health facility and that the probability of seeking care among those living in the village where the MRC is located is 100%. With this care-seeking model, we generated probabilities of attending the health facility for villages around the MRC. These probabilities were then used to

down-weight village-level population estimates derived from the WorldPop Project (63) to generate catchment area populations.

For spatio-temporal modeling, we aggregated monthly malaria incidence to the parish level (administrative level 6). Monthly incidence was defined as the count of laboratory-confirmed malaria cases from each parish within an MRC's catchment divided by the down-weighted parish-level population estimate.

Spatial Aggregation of Covariates

To aggregate raster data to the parish-level, we weighted raster values using a two-step process. First, we generated village-level population-weighted covariate estimates by weighting raster values by human population estimates from WorldPop within each village, due to the fact that malaria transmission occurs in human-dominated areas (63). Second, we generated parish-level covariate estimates by applying an additional weight derived from the care seeking model described above. Hence, the covariate values in villages demonstrating a lower probability of attending the MRC within a given parish were assigned a smaller weight than in villages demonstrating higher probabilities of attendance within that same parish.

Prior to model specification, all covariates were standardized to have a mean of 0 and a standard deviation of 1. For variables with a long-tailed distribution such as nighttime lights and distance from road, log transformation was performed prior to normalization.

Spatio-Temporal Generalized Additive Model

The number of positive cases in parish *v* at month *t* ($Y_{v,t}$) was modeled via a negative binomial generalized additive regression model (GAM) with spatio-temporal smooths accounting for a spatial latent process varying with time (64). Parish-level population denominators derived from the care seeking model ($Popseek_{v,t}$) were included as an offset term in the incidence model. A non-linear temporal trend was included with a smoothing function on month, $f(t)$. Spatio-temporal smooths were estimated using Gaussian Markov random fields (GMRF) $f(t, parish)$, allowing smooths to differ flexibly over space (parish) and time. GMRF are used to account for spatio-temporal autocorrelation when spatial data are measured over discrete polygons (65). All environmental, socio-demographic, and intervention variables were modeled with restricted cubic splines in $f(i_{v,t})$.

$$Y_{v,t} \sim NegBin(E[Y_{v,t}])$$

$$\log(E[Y_{v,t}]) = \beta_0 + f(t) + f(t, parish) + f(i_{v,t}) + offset(\log(Popseek_{v,t}))$$

Covariate selection was conducted via a two-step process. First, collinearity among all candidate covariates was assessed by calculating variance inflation factors (VIF) using a linear model including all covariates. A stepwise selection of variables with VIF < 10 was then conducted, sequentially removing the variable with the highest VIF (if the VIF ≥ 10) until all VIF < 10. Second, during GAM specification, regularization was used to integrate model selection into the model fitting step by adding an extra penalty to each term. This was performed so that coefficients for covariates can be penalized to zero, meaning that splines can be kept minimal if the data do not support flexibility (64).

Using the final model, malaria incidence aggregated to the 2-year study window was predicted at the parish level for all parishes in Uganda (n=7,569). Parish-level estimated incidence was then mapped, in addition to upper and lower bounds of 95% confidence intervals and mean standard errors across the 24-month period.

Model Validation

Model validation was conducted through cross validation. Data were split into 10 folds based on 200 km spatial blocks (see **Appendix Figure 2.1** for spatial fold distribution). Validation was assessed by comparing the estimated log counts of cases to observed log counts graphically and spatially by calculating goodness-of-fit measures including root mean squared error, mean absolute error, and R-squared.

Results

Catchment Areas

Across the 74 sites, catchment areas included between 1 and 8 parishes. The median catchment area population size was 8,054 individuals (IQR 4,451-14,048). **Appendix Table 2.1** contains site-level information on the number of parishes included in each catchment area, in addition to the population estimate of each catchment area using estimates from Afripop and malaria incidence across the 24-month study period at each site.

Distribution of Outcome and Predictor Variables

Figure 2 shows the distribution of malaria incidence at the parish level over time. At the site level, malaria incidence averaged 741 cases per 1000 person-years over 24 months. There was

substantial variation in malaria incidence over the 24-month period between sites (**Figure 2.2A**), ranging from 4 cases per 1000 person-years to 4738 cases per 1000 person-years. At the parish level (**Figure 2.2B**), monthly malaria incidence averaged 710 cases per 1000 person-years (range 0 to 11166 cases per 1000 person-years).

Figure 2.2 also shows the distribution of dynamic and static variables at the parish level. Dynamic variables include precipitation, enhanced vegetation index (EVI), daytime temperature, and nighttime temperature. All dynamic variables demonstrated some degree of seasonality: January and February were generally hotter and dryer, with wetter and cooler months June through December. Static variables also demonstrated variability across parishes. A median of 8.5% of households in each parish had improved housing (inter-quartile range [IQR] 6.8%-10.7%). Parishes were a median of 1.14 kilometers from major roads (IQR 0.17-7.96) and 12.2 kilometers from water (IQR 5.5-18.6). Parish-level population density had a median of 272 persons per 100 meters (IQR 168-353). Median slope was 1.64 degrees (IQR 1.19-2.95) and median elevation was 1078.60 meters (IQR 1054.60-1134.40). Nighttime lights across parishes were rare (77.5% of parishes <0.00001 nW/cm2/sr, indicating near-zero nighttime light emittance).

Model Fit and Validation

Model fit statistics are shown in **Appendix Figure 2.3**. There were no violations of the assumption of normality for model residuals. The R-squared of the model across all parish-months was 0.72. Results from blocked cross-validation are shown in **Appendix Figure 2.4**, comparing the R-squared of predictions in the full sample and in the cross-validated sample. In

parish-month predictions, the R-squared comparing the full to cross-validated predictions decreased from 0.72 to 0.39. On average, cases were overestimated by a factor of 1.47. When aggregating the predictions over 24 months to the parish level, the R-squared decreased from 0.84 to 0.57; cases were overestimated by an average factor of 1.32. Maps of cross-validated results showing the relative difference between estimated and observed incidence aggregated over time are shown in **Appendix Figure 2.5**.

Model Results

To estimate the relationship between predictor variables and malaria incidence, we specified a spatio-temporal GAM with Gaussian Markov Random Field smooths to account for spatial autocorrelation. Smoothed relationships from the final spatio-temporal GAM are shown in **Appendix Figure 2.2**. The final model included precipitation and nighttime temperature at 0, 1, 2 and 3 month lags, daytime temperature at 0 and 3 month lags, and EVI at 0, 1, and 3 month lags, selected by assessing collinearity and excluding variables with VIF > 10. Overall, malaria incidence increased over the 24-month study period as indicated by the monthly temporal smooth. EVI at 0 and 1 month lags were positively associated with incidence in this dataset, while EVI at a 3 month lag displayed a negative association. Overall, precipitation did not appear to be associated with incidence in this dataset. Sociodemographic covariates such as improved housing, distance from road, and distance from water, nighttime lights, and population density all demonstrated significant associations with incidence, as did elevation and slope.

Figure 2.3 shows the parish-level map of malaria risk resulting from the spatio-temporal GAM. Estimated malaria incidence was generally highest in the north, except for an area in the

Northeast that was undergoing sustained IRS since 2014 (outlined in grey). Estimates had greater certainty (narrower confidence intervals) in areas with more MRCs, particularly in the north of the country. Estimates were less stable in the southeast, where only 2 MRCs were present.

Comparison of estimates to other metrics of malaria burden

A comparison of case counts reported by the Ugandan HMIS to modeled case counts at the district level in 2019 and 2020 is plotted and mapped in **Figures 2.4A and 2.4C**. In sum, the spatio-temporal GAM estimated 40,166,418 cases of malaria across 24 months; 27,707,794 cases were reported by the HMIS in the same period. The correlation between modeled and reported case counts for each district was 0.61 ($p<0.0001$). In the majority of districts, predicted case counts were higher than HMIS-reported counts (**Figure 2.4C**); however, in some areas, particularly in the Northwest of the country, HMIS cases were higher than modeled cases.

We also compared district-level incidence in 2019 modeled by the Malaria Atlas Project (MAP) (by calculating the average mapped incidence within each district) to district-level incidence resulting from our model (Figure 4B and 4D). The correlation between these measures is 0.49 ($p<0.0001$). Across most of the higher burden North and East of Uganda, our modeled incidence is higher than MAP incidence (Figure 4D). One key exception is the 14 districts undergoing IRS in the Northeast of the country, where MAP incidence was higher than our modeled incidence. In the lower burden Southwest of the country, our modeled incidence is lower than MAP incidence. In summary, our modeled incidence appears higher than MAP incidence in higher burden areas, and lower than MAP incidence in lower burden areas.

Counterfactual scenarios

One potential use case for locally accurate risk maps of malaria incidence is the estimation of the impact of vector control interventions by modeling counterfactual scenarios. An example of this is shown in **Figure 2.5**, where we modeled malaria incidence in 2019-2020 in the 14 districts that have undergone sustained IRS since 2014. **Figure 2.5A** shows the predicted incidence under sustained IRS, while **Figure 2.5B** shows the predicted incidence under the counterfactual scenario of no IRS. The model suggests that approximately 5 million cases were averted across the 24-month period (1,046,402 cases in the IRS scenario, 6,310,209 cases in the non IRS scenario). The difference between the estimated counterfactual incidence and estimated incidence under IRS was greater in districts in the north, where transmission is higher.

Discussion

This study used routinely collected data from 74 health facilities to estimate, model, and map malaria incidence and its uncertainty in Uganda. Our findings indicate that individual-level, high quality patient data collected at a limited number of sentinel health facilities across a geographic area represent a potential avenue for generating high resolution maps of malaria risk with the potential for operational utility. While the maps we generated were less informative in areas distant from sentinel surveillance sites, estimates were stable in areas with a higher density of sites, particularly in the north and northeast of Uganda. These maps shed light on potential underreporting of cases from the HMIS and on the impact of IRS in districts receiving regular IRS campaigns.

Over the past several years, the steady decline of malaria cases and deaths that has taken place since the 1990s has stalled, particularly in high burden countries like Uganda (41). Given this, in

combination with the heterogeneous nature of malaria transmission, NMCPs must have high quality information to maximize limited resources by targeting vector control approaches and evaluating their impact. Locally informed, contemporaneous maps of malaria risk represent a potential source of this information. At present, most malaria risk mapping is done using cross-sectional surveys capturing parasite prevalence, such as Malaria Indicator Surveys or Demographic and Health Surveys. These surveys are conducted infrequently (typically, every 3-5 years) and are limited in geographic scope. Furthermore, while parasite prevalence as a metric may be related to malaria burden, it has less programmatic relevance than more direct indicators such as malaria incidence (44). To compensate for this, methods to estimate incidence using cartographic tools linking parasite prevalence to incidence have been recently developed by the Malaria Atlas Project (8, 9). While these methods improve the operational utility of risk maps by converting prevalence to a more meaningful surveillance measure, they lack both accuracy and precision because the relationship between prevalence and incidence is poorly defined and inconsistent, especially in areas where transmission intensity is high (41). For this reason, a recent push by the World Health Organization's High Burden to High Impact initiative has focused on leveraging HMIS for surveillance and risk mapping (41). However, this comes with its own challenges. First, quality surveillance requires accurate diagnosis, yet only 38% of febrile children brought for care at a public health facility received a diagnostic test in 2015-2019 (41). Second, once cases are identified, they must be reported through the HMIS, yet reporting rates vary significantly and cases are often reported in aggregate (41). Third, even under conditions of high quality HMIS data, translating raw case numbers into meaningful indicators of disease burden is challenging because catchment areas around health facilities are not well defined.

This study proposes potential solutions for each of these challenges. First, our dataset had high spatial and temporal resolution for much of Uganda, particularly in comparison with cross-sectional surveys typically used for risk mapping purposes. We continuously collected incidence data from 310 parishes across the country over a period of 2 years. The most recent (2018-19) Malaria Indicator Survey in Uganda, in contrast, was a one-time survey conducted in 320 clusters (40). Second, we leveraged a network of enhanced HMIS sentinel sites that addresses many of the issues associated with standard HMIS systems: data are at the individual patient level, diagnostic testing rates are high (in 2019-2020, 99.6% of patients suspected of having malaria were tested), and missingness of key variables is near-zero (0.12% missingness for age, 0.07% for sex, and 4.25% missingness for village of residence in 2019-2020). Finally, using these data we translated individual-level case data to accurate measures of monthly malaria incidence by utilizing information on patients' places of residence to estimate catchment area populations (62). Compared with modeling incidence as a function of parasite prevalence, this method is a more direct and relies on fewer assumptions.

While this study focused on Uganda, this method has the potential to improve malaria surveillance at an operational level in malaria endemic settings globally. Because malaria incidence is measured directly, continuously, and locally at health facilities rather than relying on a complex mathematical model, barriers NMCP face to get relevant estimates are lower. Measures of incidence can then be combined with publicly available remotely sensed data in order to extrapolate these estimates to areas where sentinel sites are not present. The higher density of sentinel surveillance sites that are included, the fewer modeling assumptions would be needed because there would be fewer areas with sparse data and precision of incidence estimates

would be higher. Harnessing sentinel site data to generate maps of risk has the added operational benefit of high temporal resolution, meaning that NMCP can use these maps to track changes in burden over time and estimate the impact of control interventions by modeling counterfactual scenarios.

This analysis is not without limitations. First, health facility data are limited to information recorded for patients that visit that health facility. While our incidence estimates do adjust for care-seeking as a function of distance to the facility, we do not adjust for probabilities of care-seeking for reasons other than distance. However, if this were of interest, these data could be combined with survey data on care-seeking. For example, in the villages adjacent to a subset of MRCs, cross-sectional surveys were conducted in April 2021; these surveys found that 67% of survey participants with fevers in previous 2 weeks sought care at the MRC. Because these villages were very close to the MRC (and therefore travel time should be negligible), we could apply an additional assumption that our model captures only 67% of true cases in Uganda. This would further the gap between estimated cases and cases reported by the HMIS, suggesting that HMIS data may be substantially underestimating burden. Second, despite being inexpensive relative to cross-sectional surveys, sentinel surveillance systems do require some investment compared with standard HMIS data, including additional time and labor associated with inputting individual-level patient data to a digital database. Furthermore, an initial investment is needed to accurately record where patients reside and to link these areas of residence to places on a map. Third, we rely on modeling assumptions that may be incorrect. For example, we rely on data from 74 health facilities in combination with covariate information to extrapolate malaria burden to the rest of the country, meaning that in areas with lower density of MRCs, our

estimates had greater uncertainty. However, the relatively low cost of adding more sentinel surveillance sites could greatly diminish the potential inaccuracy of these modeling assumptions and vastly improve these maps across the entire country.

Despite these limitations, this proposed method may be of interest to NMCPs given the benefits of measuring and mapping malaria incidence locally and contemporaneously. In order to establish a robust system to estimate and map malaria burden, local stakeholders could establish a network of high-quality HMIS surveillance sites. Although a larger number of sites would have greater operational benefit, local NMCPs may select the number and distribution of sites based on local need and factors influence decision making (for example, if vector control interventions are typically implemented at the district level, 1 site per district may suffice). At these sites, individual-level data on a few key indicators including demographics, place of residence, and malaria diagnostics – all of which are standard patient information in many public health facilities – could be collected. Using information on patient residence, population denominators accounting for care seeking may be estimated, or, alternatively and more simply, catchment areas could be defined including patients living immediately around the health facility where care-seeking can be assumed to be maximal. With this information, enhanced HMIS surveillance data can be used to generate quality measures of malaria incidence that can then be extrapolated to other areas of the country through simple spatial smoothing or by combining this information with spatial covariates. This proposed methodology represents a "best of both worlds," allowing for high-quality, local surveillance data to be collected and mapped contemporaneously at a low cost with minimal additional labor required. Risk maps generated using this method have the

potential to be an essential tool for high burden countries around the globe as they aim to achieve targets toward control and elimination.

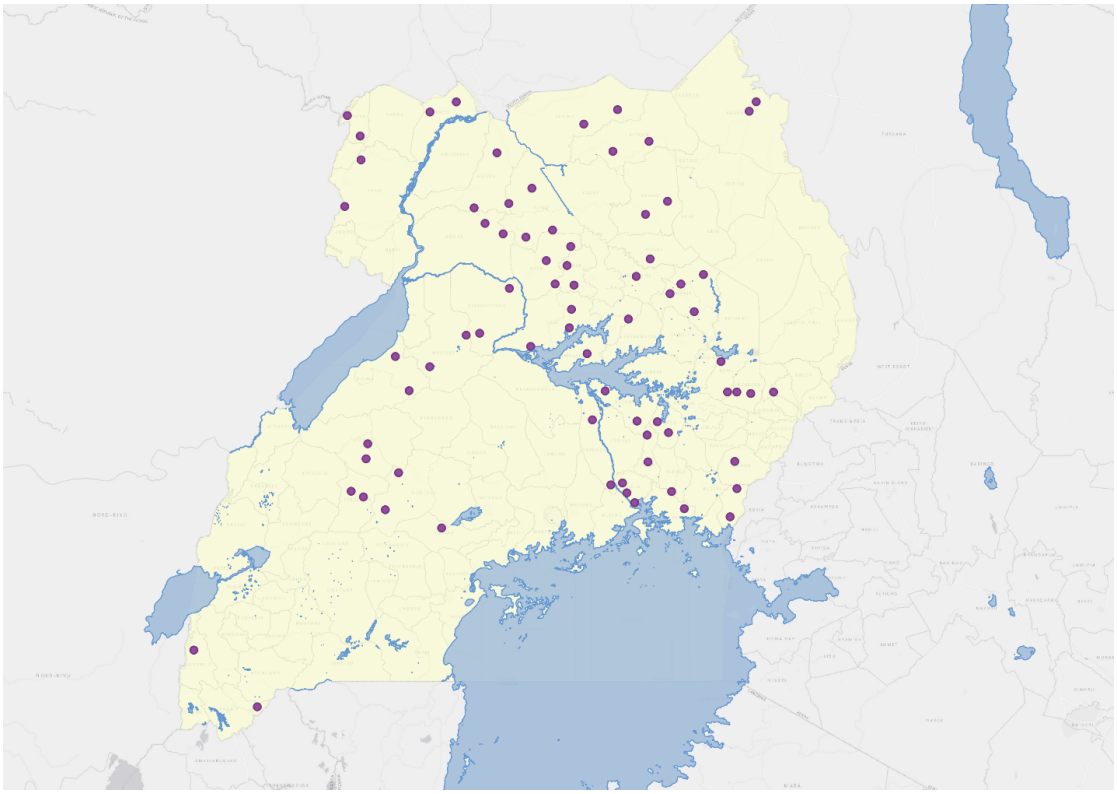

Figure 2.1. Map of Malaria Reference Centers included in risk mapping analysis.

Table 2.1. Candidate covariates for spatio-temporal generalized additive model.

Covariate	Description	Temporal Status	Source	Available Resolution
precip	Cumulative monthly precipitation	Monthly; 0, 1, 2, 3 month lags	CHIRPS	0.05 decimal degrees
lst_day	Daytime land surface temperature	Monthly; 0, 1, 2, 3 month lags	MODIS derivative	1 kilometer
lst_night	Nighttime land surface temperature	Monthly; 0, 1, 2, 3 month lags	MODIS derivative	1 kilometer
evi	Enhanced vegetation index	Monthly; 0, 1, 2, 3 month lags	MODIS derivative	1 kilometer
elevation	Elevation as measured by the Shuttle Radar Topography Mission (SRTM)	Static	Shuttle Radar Topography Mission	90 meter
slope		Static	WorldPop	100 meter
pop_density	Population density per grid-cell	Static	WorldPop	100 meter
dist_road	Distance to OpenStreetMap major roads (in km)	Static	WorldPop	100 meter
dist_water	Distance to OpenStreetMap major waterways (in km)	Static	WorldPop	100 meter
housing	Prevalence of improved housing	Static	Malaria Atlas Project	1 kilometer
nighttime_lights	Index that measures the presence of nighttime lights from towns and cities	Static	VIIRS	500 meters
irs	Number of months since last IRS campaign*binary variable indicating IRS district	Monthly	Uganda NMCP	District level
llin	Number of months since last LLIN distribution	Monthly	Uganda NMCP	District level

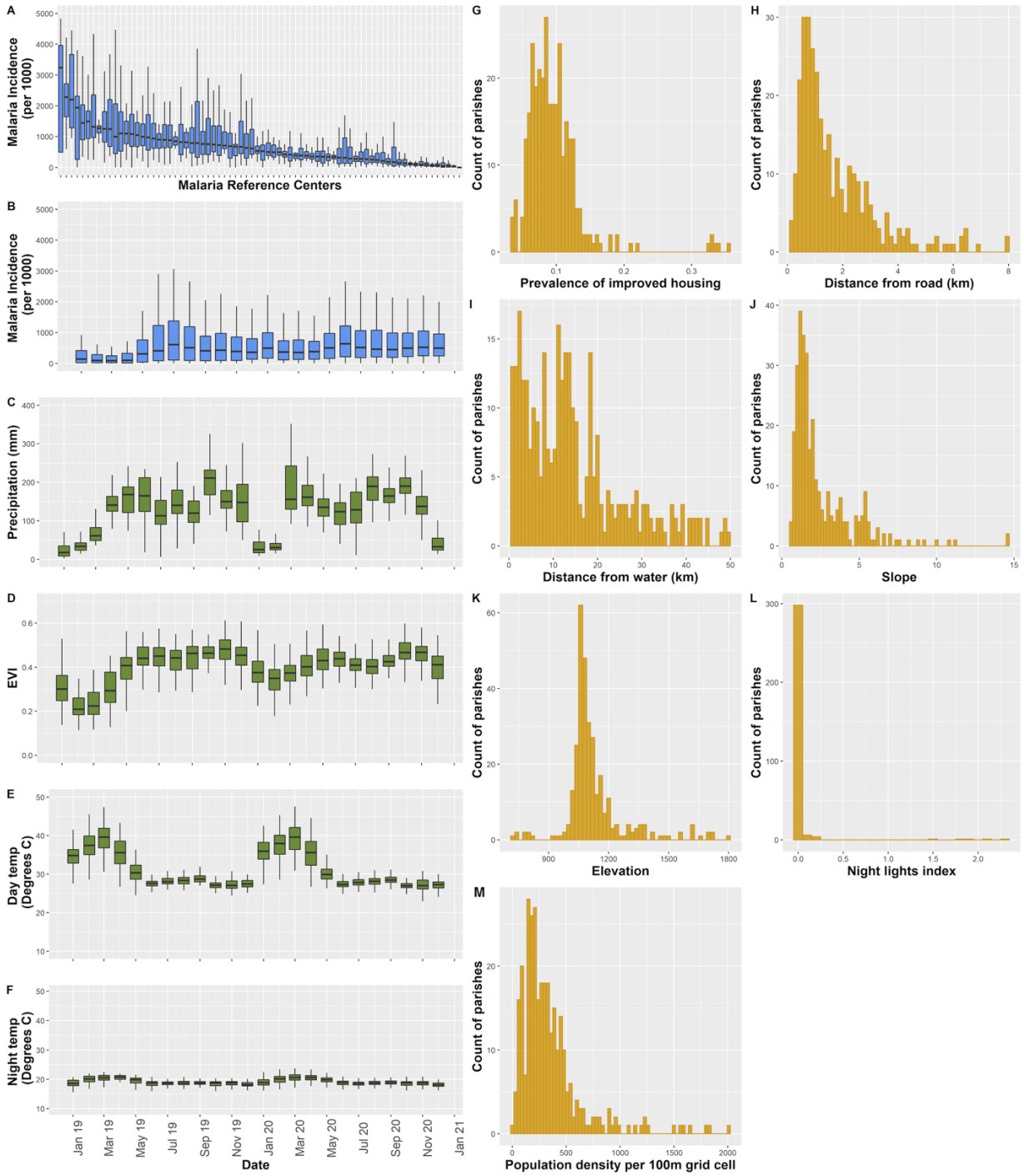

Figure 2.2. Distribution of outcome (malaria incidence) (A) between sites and (B) over time and of dynamic predictor variables at the parish level for dynamic covariates (C-F) and static covariates (G-M). Lags of 0, 1, 2, and 3 months were considered for dynamic covariates.

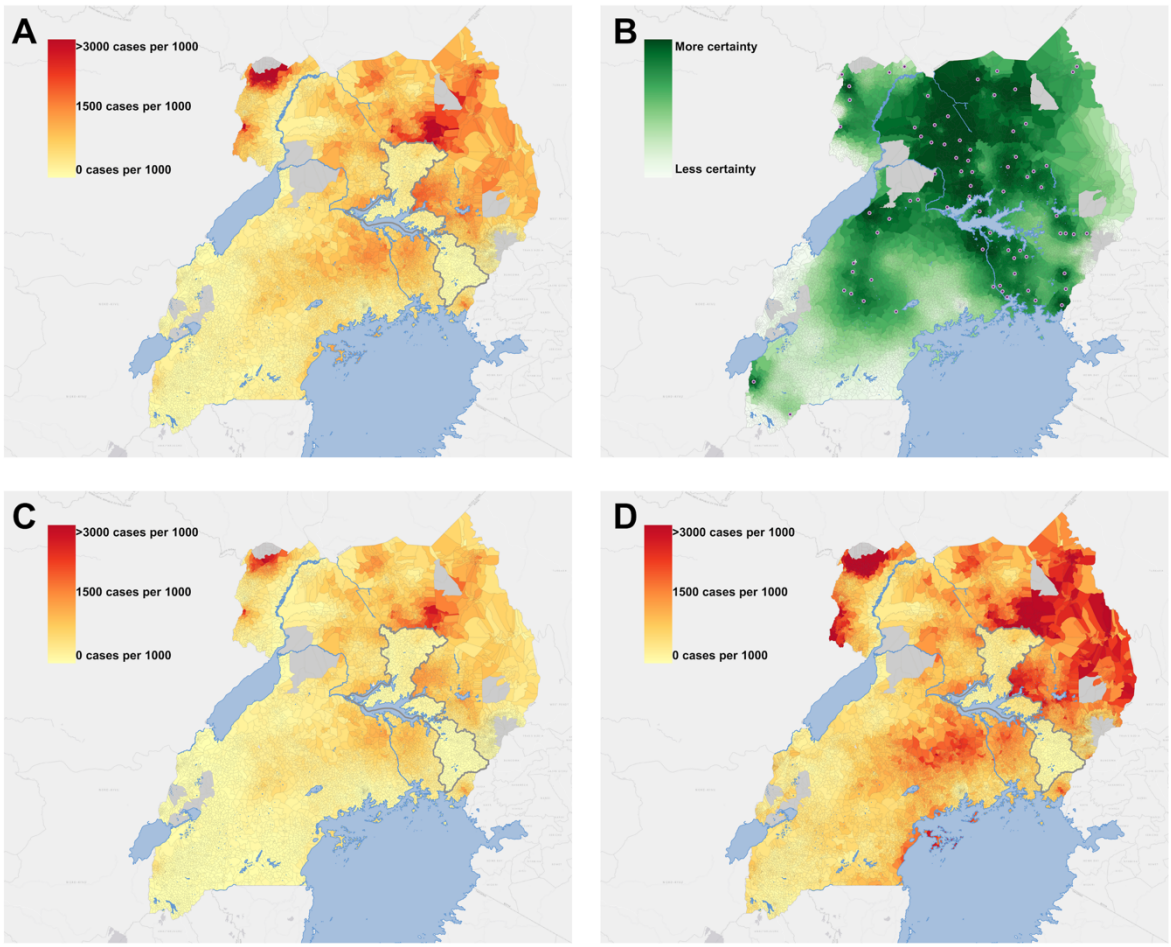

Figure 2.3. A) Parish-level estimated incidence per 1000 over the study window; B) mean standard error on the log scale and locations of Malaria Reference Centers; C) lower and D) upper bound of the 95% confidence interval. Districts receiving indoor residual spraying campaigns are outlined in grey in panels A, C, and D.

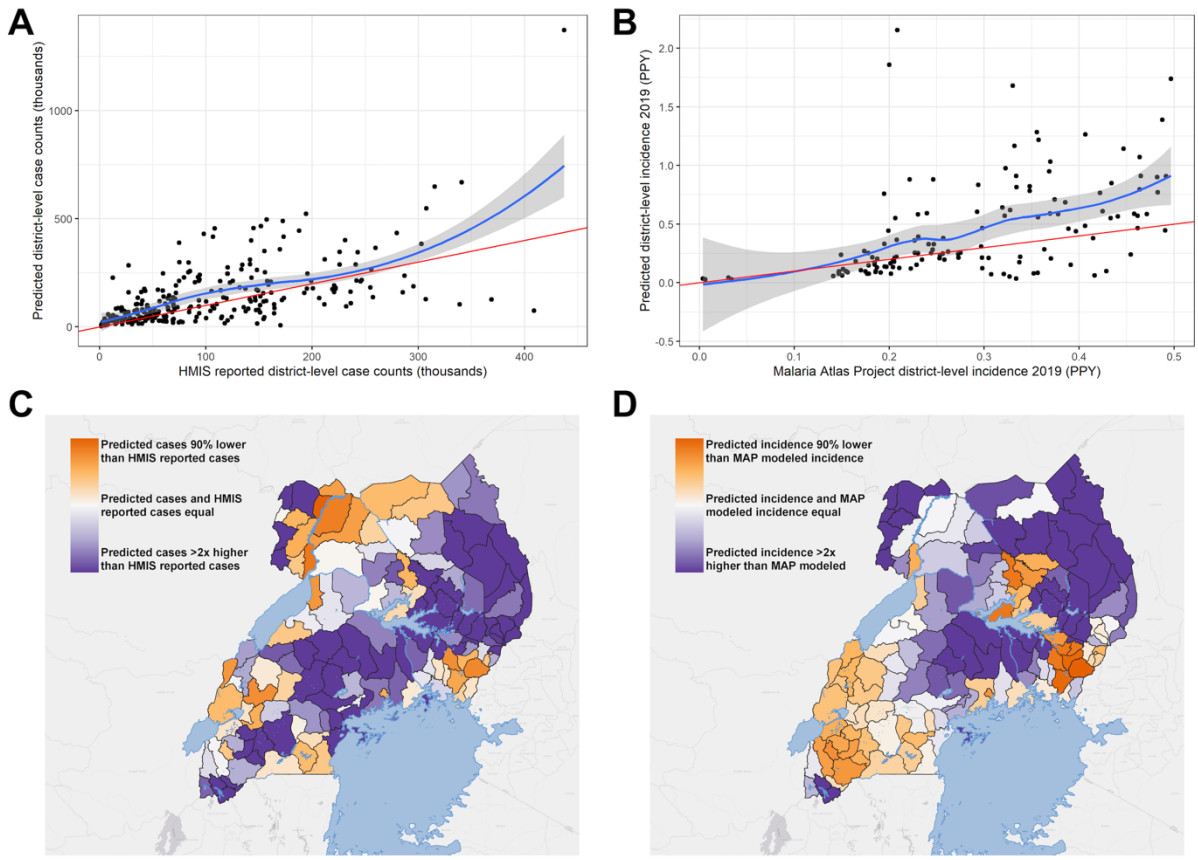

Figure 2.4. A) Comparison of district-level case counts reported by the Ugandan HMIS to estimated district-level case counts in thousand in 2019 and 2020; B) comparison of district-level average malaria incidence modeled by the Malaria Atlas Project to estimated district-level incidence in 2019; C) mapped district-level differences in case counts reported by the Ugandan HMIS to estimated district-level case counts in thousand in 2019 and 2020; D) mapped district-level differences in average malaria incidence modeled by the Malaria Atlas Project to estimated district-level incidence in 2019. The identity line in panels A and B is indicated in red and a lowess smooth is indicated in blue.

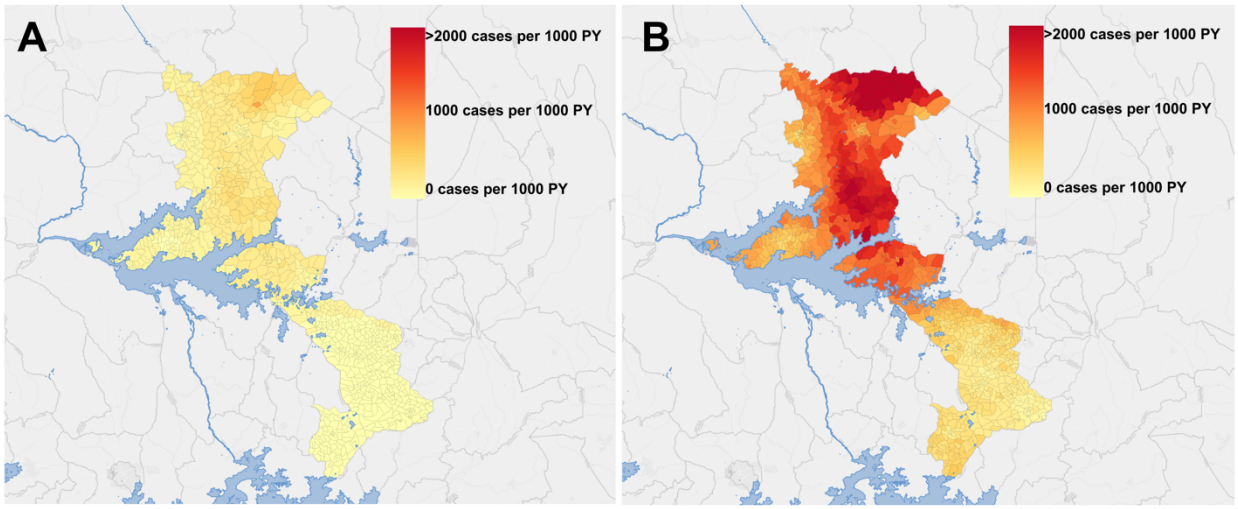

Figure 2.5. Predicted malaria incidence in 14 districts undergoing indoor residual spraying in 2019-2020 under A) true IRS conditions and B) counterfactual IRS conditions with no IRS.

Chapter 2 Appendix

Appendix Table 2.1. Descriptive information on Malaria Reference Centers included in spatio-temporal model.

District	Site	Number of months of data observed	Number of parishes included in catchment area	Population of catchment area	Number of laboratory confirmed cases of malaria	Malaria incidence (per 1000)
Agago	Lira-Kato	13	3	1869	9594	4738
Agago	Patongo	24	3	7092	13476	950
Alebtong	Alebtong	23	6	8777	2001	119
Amolatar	Amolatar	24	7	12630	1892	75
Amuria	Asamuk	12	7	7727	7479	968
Amuria	Morungatuny	11	5	6860	4518	718
Amuru	Amuru	14	4	36831	2456	57
Amuru	Atiak	18	6	17474	15896	606
Apac	Aduku	24	5	16957	14240	420
Apac	Akokoro	10	2	1214	2597	2567
Apac	Teboke	11	5	20695	4837	255
Arua	Cilio	13	4	8390	3172	349
Arua	Opia	24	3	3615	14862	2056
Bukedea	Bukedea	4	4	1046	469	1345
Bukedea	Kolir	14	3	3530	2798	679
Busia	Busitema	10	4	10820	4650	516
Busia	Lumino	24	5	6058	12003	991
Buyende	Bugaya	11	4	4289	5780	1470
Buyende	Kidera	8	4	22835	5583	367
Dokolo	Dokolo	14	5	13874	5395	333
Gomba	Maddu	11	4	8184	865	115
Gulu	Awach	24	6	30035	24279	404
Gulu	Pabwo	10	2	5465	4247	933
Hoima	Butema	11	7	16330	947	63
Hoima	Kigorobya	24	8	23707	8857	187
Jinja	Budondo	11	3	4738	1729	398
Jinja	Butagaya	12	2	2887	1658	574
Jinja	Walukuba	12	2	3276	1314	401
Kaabong	Kalapata	11	5	4961	5681	1249
Kaabong	Lokolia	19	2	1027	3887	2390
Kaliro	Bumanya	10	5	16691	2678	193
Kaliro	Nawaikoke	10	4	2393	2728	1368
Kanungu	Kihihi	24	8	8180	5833	357
Kapchorwa	Kaserem	12	5	2250	146	65
Kapelebyong	Kapelebyong	14	1	4356	3445	678
Kapelebyong	Obalanga	12	7	18863	7990	424
Kayunga	Bbaale	24	6	6191	12602	1018
Kayunga	Kangulumira	10	5	14071	5468	466
Kibaale	Kibaale	10	8	8580	935	131
Kibaale	Kyebando	11	5	7243	3459	521
Kiryandongo	Diima	10	2	6268	5473	1048
Kiryandongo	Kigumba	11	3	4897	1612	359
Kitgum	Kitgum_Matidi	14	1	5125	4611	771
Kitgum	Namokora	24	4	13979	9056	324
Koboko	Ayipe	13	2	3594	4004	1028

District	Site	Number of months of data observed	Number of parishes included in catchment area	Population of catchment area	Number of laboratory confirmed cases of malaria	Malaria incidence (per 1000)
Koboko	Lobule	24	6	8731	23164	1327
Kole	Aboke	11	2	5318	4483	920
Kole	Bala	6	5	13870	3691	532
Kumi	Kamaca	10	4	38648	10679	332
Kumi	Omatenga	13	5	9542	14714	1423
Kwania	Apwori	14	3	7930	9357	1011
Kyegegwa	Kakabara	12	5	21029	2448	116
Kyegegwa	Kyegegwa	11	4	16948	1215	78
Lamwo	Madi Opei	10	4	11089	7077	766
Lamwo	Padibe	24	5	6278	13895	1107
Luuka	Ikumbya	12	4	5453	6690	1227
Luuka	Kiyunga	10	3	15049	4667	372
Masindi	Bwijanga	10	3	10430	884	102
Masindi	Kyatiri	10	1	1537	234	183
Mayuge	Buwaiswa	12	5	11905	5261	442
Mayuge	Kigandolo	11	6	21561	4013	203
Moyo	Lefori	4	2	3381	1386	1230
Moyo	Metu	4	4	6281	1706	815
Mubende	Kasambya	24	1	1113	945	425
Mubende	Kiyuni	11	2	5045	1481	320
Nwoya	Alero	9	3	9135	4207	614
Nwoya	Koch Goma	17	4	16481	19822	849
Omoro	Bobi	11	3	3832	7228	2058
Omoro	Lalogi	24	5	15326	19431	634
Otuke	Orum	24	2	210	309	736
Oyam	Anyeke	24	4	14943	11046	370
Oyam	Otwal	14	6	3989	7523	1617
Rukiga	Kamwezi	11	6	11892	48	4
Tororo	Nagongera	24	7	13906	842	30

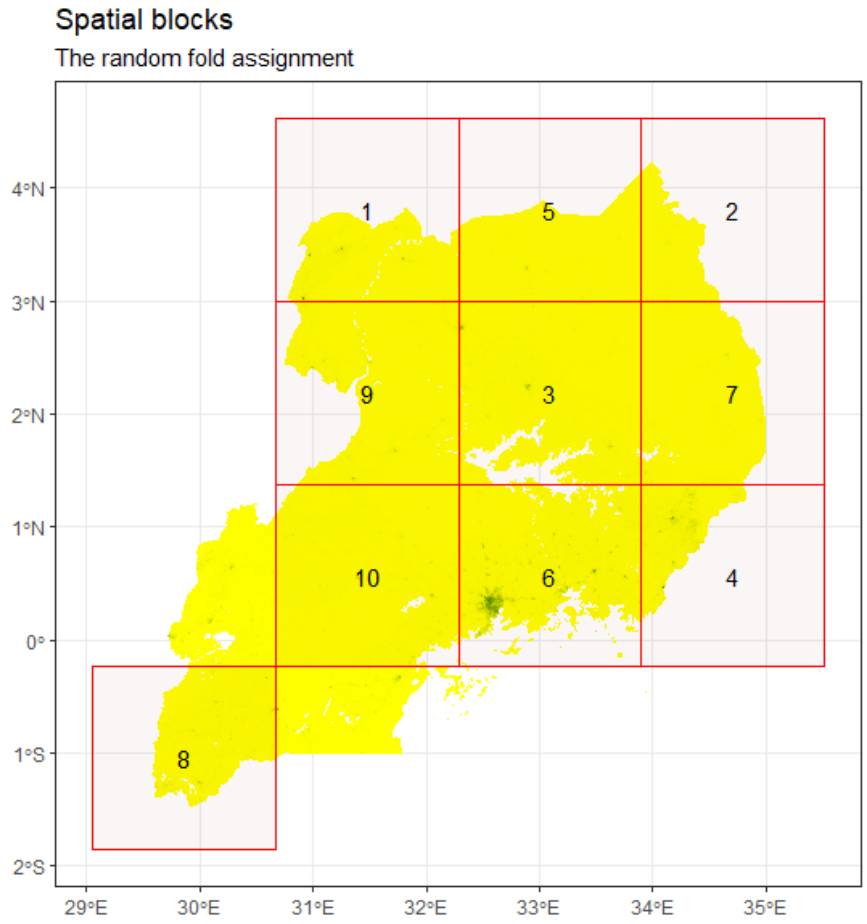

Appendix Figure 2.1: Map of spatial blocks of 200km for cross validation.

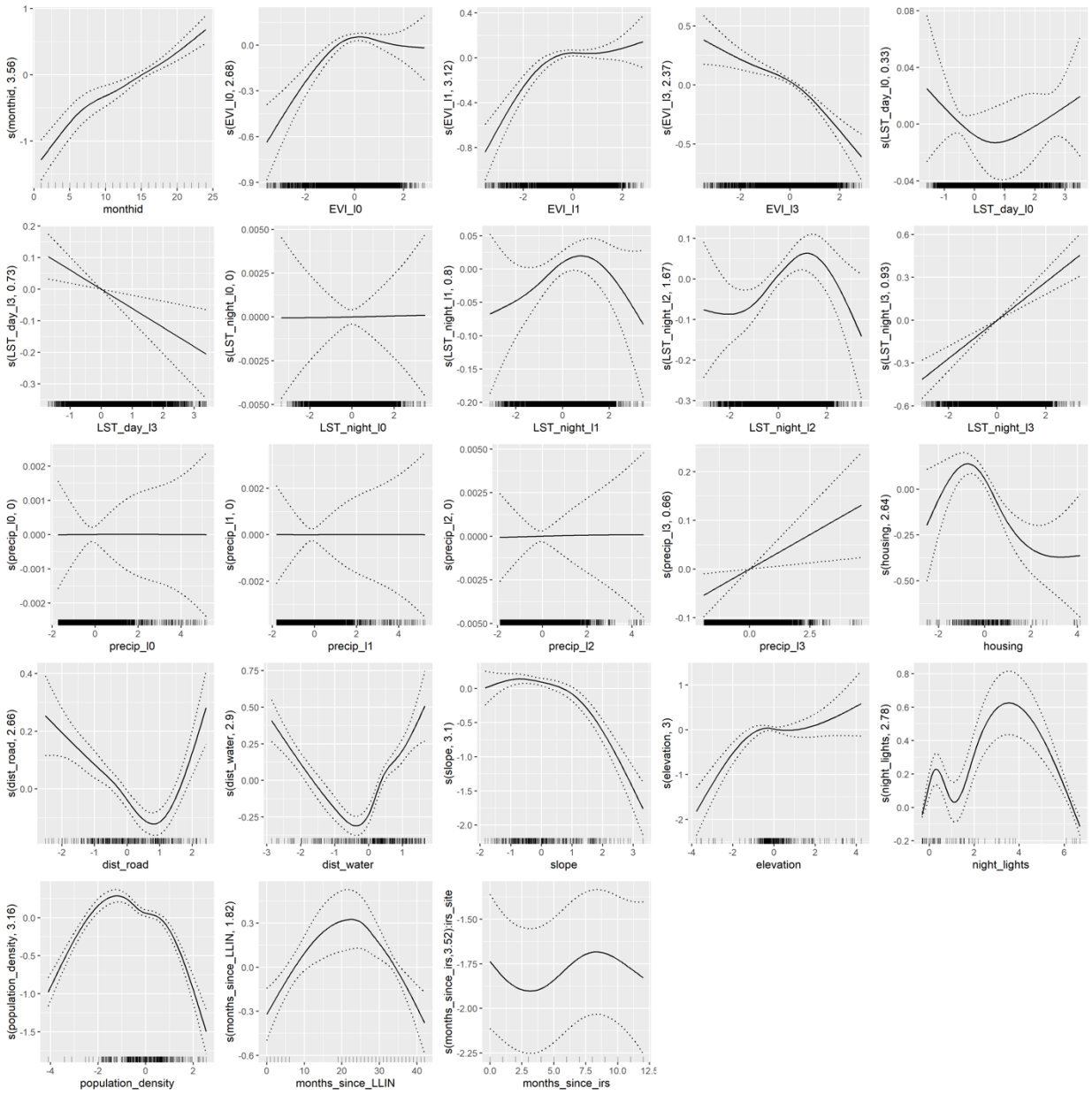

Appendix Figure 2.2. Smoothed relationships between covariates and outcome.

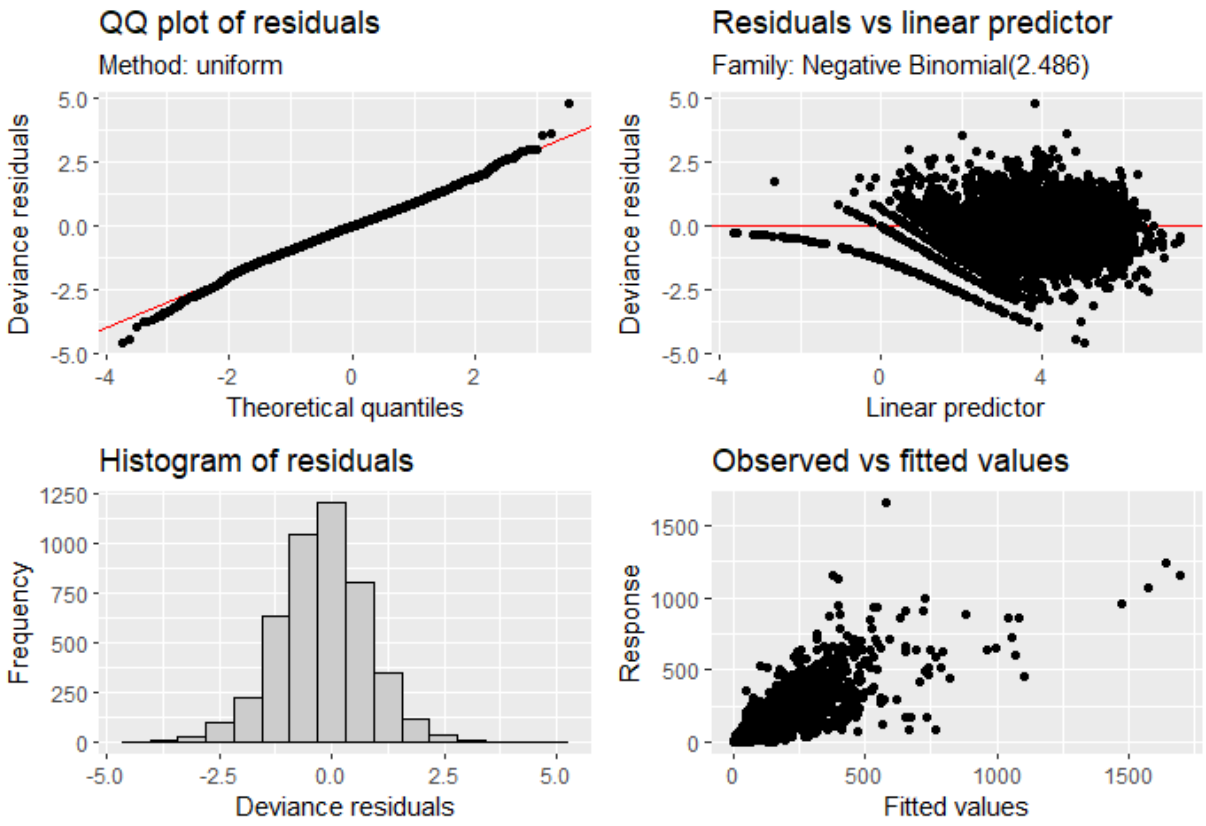

Appendix Figure 2.3: Model diagnostics from generalized additive model.

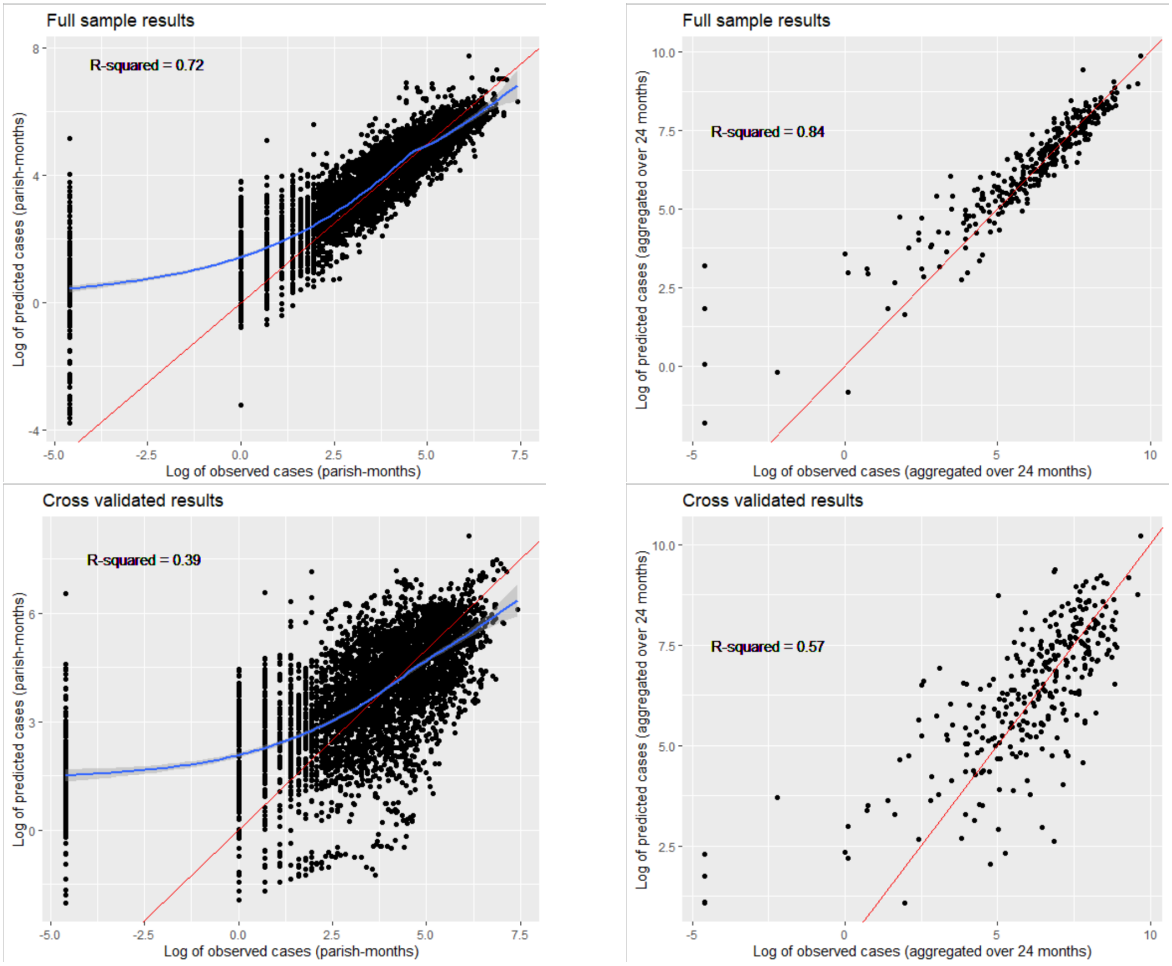

Appendix Figure 2.4. Results of cross validation.

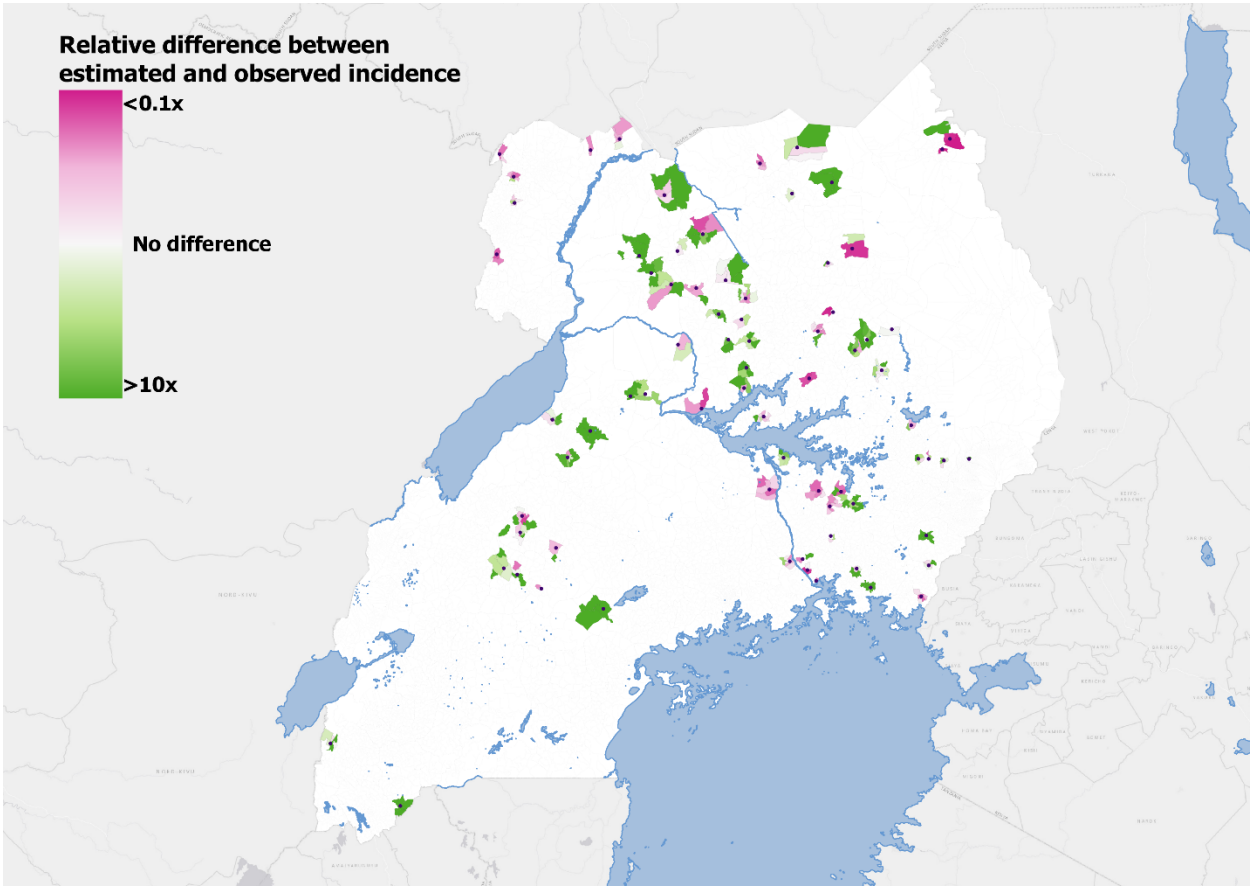

Appendix Figure 2.5. Mapped results of cross validation.

Chapter 3: Resurgence of malaria burden in five districts in Uganda despite sustained indoor residual spraying and repeated long lasting insecticidal net distributions

Adrienne Epstein, Catherine Maiteki-Ssebuguzi, Jane F. Namuganga, Joaniter I. Nankabirwa, Samuel Gonahasa, Jimmy Opigo, Sarah G. Staedke, Josephat Shililu, Michael Okia, Asaph Muhanguzi, Mame Niang, Damian Rutazaana, Emmanuel Arinaitwe, Kassahun Belay, Moses R. Kamya, Samir Bhatt, Isabel Rodriquez-Barraquer, Bryan Greenhouse, Martin J. Donnelly, Grant Dorsey

Abstract

Background

Five years of sustained indoor residual spraying of insecticide (IRS) from 2014 to 2019, first using a carbamate followed by an organophosphate, was associated with a marked reduction in the burden of malaria in five districts of Uganda. We assessed malaria burden over an additional 18 months, corresponding to a change in IRS formulations using clothianidin with and without deltamethrin.

Methods

Our objectives were: 1) to estimate the impact of IRS on monthly malaria case counts at five health facilities over a 6·5 year period, and 2) to compare monthly case counts at five facilities receiving IRS to ten facilities in neighboring districts not receiving IRS. For both objectives, we specified mixed effects negative binomial regression models with random intercepts for health facility adjusting for rainfall, season, care-seeking, and test type.

Results

Following the implementation of IRS, cases were 84% lower in years 4-5 (adjusted incidence rate ratio [aIRR]=0.16, 95% CI 0.13-0.20), 43% lower in year 6 (aIRR=0.57, 95% CI 0.45-0.72),

and 25% higher in the first 6 months of year 7 (aIRR=1.25, 95% CI 0.93-1.69) compared to pre-IRS levels. Cases were 69% lower in IRS sites than non-IRS sites in year 6 (aIRR=0.31, 95% CI 0.19-0.51) but 20% higher in the first 6 months of year 7 (aIRR=1.20, 95% CI 0.2-2·00).

Conclusions

We observed a resurgence in malaria to pre-IRS levels despite sustained IRS. The timing of the resurgence corresponded to a change of active ingredient used in IRS. Future work is needed to determine causality.

Introduction

Major gains have been made in reducing the burden of malaria in sub-Saharan Africa over the past two decades, resulting in a 44% decline in malaria deaths between 2000 in 2019 (9, 41). However, progress has slowed in recent years, particularly in highest burden countries (41). Much of the decline in malaria burden has been attributed to vector control interventions, including long-lasting insecticidal nets (LLINs) and indoor residual spraying of insecticide (IRS). Scale-up of LLINs coverage has occurred rapidly, with the proportion of households in sub-Saharan Africa with at least one LLIN increasing from 5% in 2000 to 68% in 2019 (41). Conversely, the percent of at-risk populations receiving IRS has been much lower and even declined from 5% in 2010 to 2% in 2019 (41). Challenges to the scale-up of IRS coverage include high cost, complex implementation logistics, and community acceptance (66). Furthermore, evidence from controlled trials is mixed on the added benefit of implementing IRS in communities where LLIN coverage is high (67).

Uganda is illustrative of high burden countries where progress in reducing malaria burden has slowed in recent years (41). The Ugandan Ministry of Health has made a strong commitment to ensuring high LLIN coverage, delivering LLINS through 3 universal coverage campaigns (UCC) taking place in 2013-2014, 2017-2018, and 2020-21. These campaigns have been successful: in 2018-2019, 83% of households reported owning at least one LLIN, the highest coverage globally (40). IRS was reintroduced into Uganda in 2006 for the first time since the 1960s and coverage of IRS to date has been much lower than LLINs. From 2007 to 2014, IRS was implemented in 10 districts in Northern Uganda before being moved to 14 historically high burden districts in North-Eastern Uganda in 2014. The IRS campaign in the northeast initially deployed a

carbamate insecticide before changing to an organophosphate for the third, fourth, and fifth years. In this part of the country, IRS has been considered highly successful: in the first 3 years of sustained IRS campaigns, malaria cases at sentinel surveillance sites in 5 of these districts fell by 50%, and in the fourth and fifth years, by 85% compared to pre-IRS levels (50).

In this study, we use data from a network of health facility-based malaria surveillance sites to examine the impact of sustained IRS in the 5 districts mentioned above. This study has two objectives. First (Objective 1), we extend our prior analysis to evaluate the malaria burden in 5 districts receiving IRS in the 6th and 7th years of sustained IRS (January 2020 through July 2021) relative to a baseline period before IRS was initiated. This extended evaluation period coincided with a shift in insecticide formulations from the organophosphate pirimiphos-methyl (Actellic 300CS®) to products containing the active ingredient clothianidin alone (Sumishield®) or combined with deltamethrin (Fludora® Fusion WP-SB), the beginning of the COVID-19 pandemic, and another LLIN universal coverage campaign (2020-2021). Second (Objective 2), we compare temporal changes in malaria burden from January 2020 through July 2021 at the 5 sites receiving sustained IRS to 10 sites in neighboring districts that have not received IRS recently.

Methods

Study sites and vector control interventions

This study utilized enhanced health facility surveillance data from 15 health facilities in Uganda: 5 located in districts that have received repeated rounds of IRS since December 2014 and 10 in neighboring districts that have never received IRS (6 sites) or where IRS was discontinued in

2017 (4 sites, **Figure 3.1**). These facilities are part of a surveillance network called the Uganda Malaria Surveillance Program (UMSP). National LLIN universal coverage campaigns were conducted in 2013-2014, 2017-2018, and 2020-2021, where LLINs were distributed free-of-charge by the Uganda Ministry of Health targeting 1 LLIN for every two household residents throughout the entire country (following WHO recommendations). During the most recent campaign (2020-2021), the Ministry of Health distributed conventional LLINs containing pyrethroid in addition to two types of "next generation" LLINs due to concerns of pyrethroid resistance: one containing deltamethrin and piperonyl butoxide (Permanet® 3.0) and one containing alpha-cypermethrin and pyriproxyfen (Royal Guard®). Among the sentinel sites included in this study, the 5 sites in IRS districts were in sub-counties that received conventional pyrethroid nets and the 10 sites in neighboring districts were in sub-counties that received "next generation" nets (5 received Permanet® 3.0 nets and 5 received Royal Guard® nets).

In the 5 study districts where IRS was first implemented in late 2014, the insecticide formulation initially consisted of a carbamate (bendiocarb) with rounds repeated approximately every 6 months until 2016 when the active ingredient was changed to the organophosphate pirimiphos-methyl (Actellic 300CS®) administered annually until 2019. In 2019, one study district (Dokolo) received a single round of IRS with Sumishield® 50WG, a new IRS product containing clothianidin. In 2020, all IRS districts began receiving IRS with Fludora® Fusion WP-SB, a new IRS insecticide containing a mixture of clothianidin and deltamethrin. Changes of IRS insecticides were made in accordance with the Ugandan Ministry of Health's insecticide resistance management plan which, in line with WHO recommendations, requires changing IRS formulations every three years to preempt the development of resistance (68, 69). In two study

districts (Otuke and Alebtong), IRS was discontinued in 2021 due to lack of funding. For a complete timeline of all IRS campaigns, including insecticides and coverage, see **Appendix Table 3.1**.

Health-facility based surveillance

A network of enhanced malaria surveillance sites embedded in public health facilities was established by UMSP in 2006, as previously described (22). In brief, UMSP currently operates Malaria Reference Centers (MRCs) – at 70 level III/IV public health facilities across Uganda. Level III and IV health facilities are parish and sub-county level facilities, respectively, and provide diagnostic testing and treatment free of charge to populations of 20,000 to 100,000 people per facility. Data are collected at the individual level for all outpatients attending MRCs using outpatient registers (HMIS 002) and entered monthly into a database by on-site data entry officers. Information collected includes sociodemographic data (age, sex, and village of residence), whether malaria was suspected, results of laboratory testing for malaria (rapid diagnostic test [RDT] or microscopy), diagnoses (laboratory-confirmed and clinical), and treatments prescribed. UMSP places emphasis on high quality data, ensuring minimal missingness on key variables including age and place of residence, and providing training and materials to maximize diagnostic testing among patients suspected of having malaria. For Objective 1 (to evaluate the malaria burden in 5 districts receiving IRS in the 6th and 7th years of sustained use), we utilized data from 5 MRCs from districts with sustained rounds of IRS since 2014. These MRCs were selected because they had been active UMSP sites for at least 6 months prior to the initiation of IRS. To compare changes in malaria burden from January 2020 through July 2021 at sites receiving sustained IRS to sites in neighboring districts that have not received

IRS recently, we used data from 10 additional MRCs. These sites were selected because they were in districts that neighbor the 5 IRS sites and have been active UMSP sites since at least January 2020. Four of these sites were in 2 districts that received IRS in the past; however, IRS was stopped in 2017. The impact of these previous IRS campaigns was no longer evident during the study period (50).

Measures

For Objective 1, the exposure was specified as an indicator variable representing each month since IRS was initiated. In separate models, a categorical variable, representing months 1-36 (years 1, 2, and 3), 37-60 (years 4 and 5), 61-72 (year 6), and 73-78 (the first 6 months of year 7) of sustained IRS was included as the primary exposure variable. The baseline period was defined as the 12 months before IRS was implemented in 2014; if a site had less than 12 months of baseline data available, we included the maximum amount of time available.

For Objective 2, the exposure was specified as a binary variable representing whether a site was an IRS site or a non-IRS site. This variable was then interacted with an indicator variable representing time (an indicator representing month/year and, in a separate model, a categorical variable representing January 2020-December 2020 and January 2021-July 2021).

For both objectives, the primary outcome was the monthly count of laboratory-confirmed malaria cases at each MRC. To correct for monthly testing rates, we adjusted this count by multiplying the number of individuals with suspected malaria but not tested each month by the test positivity rate (TPR) (the number who tested positive divided by the total number tested) in

that month. We then added the result to the number of laboratory-confirmed positive cases in that month. As a sensitivity analysis, we re-specified the models including only laboratory-confirmed case counts as the outcome.

We adjusted for time-varying variables that impact malaria burden and malaria case detection at the health facility. This includes precipitation (54) which was modeled non-linearly using restricted cubic splines. Lags of 0, 1, 2, and 3 months were considered for precipitation; the appropriate lag was selected by running univariable regressions with each lag and selecting that which demonstrated the lowest Akaike's information criterion (AIC). We also included indicator variables for month of the year (to adjust for season), the proportion of tests that were RDT (vs. microscopy) in that month, and the number of individuals who attended the health facility but were not suspected of having malaria in that month (to adjust for potential changes in care-seeking behaviors, particularly during the COVID-19 lockdown in Uganda).

Statistical analysis

For Objective 1, we specified mixed effects negative binomial regression models with random intercepts for health facility. Coefficients for the exposure variable were exponentiated to represent the incidence rate ratio (IRR) comparing the incidence of malaria in the month of interest relative to the baseline pre-IRS period. These models test the null hypothesis of no difference of changes in IRS burden after the initiation of IRS compared to before the initiation of IRS, adjusting for seasonal effects and time-varying changes in diagnostic testing and care seeking.

For Objective 2, models were specified as mixed effects negative binomial regression models with random intercepts for health facility. Coefficients for the exposure variable combined with the interaction term were exponentiated to represent the incidence rate ratio (IRR) comparing the burden of malaria IRS sites versus non-IRS sites over a given period of time. These models test the null hypothesis of no difference between malaria burden at IRS sites compared to non-IRS sites, adjusting for seasonal effects and time-varying changes in diagnostic testing and care seeking.

Results

Study Objective 1

Across the 5 sites receiving sustained IRS, a total of 740,226 outpatient visits were recorded from the baseline period covering up to 12 months before IRS started through July 2021 (**Table 3.1**). During the baseline period, average monthly cases adjusted for testing ranged from 278-657 and TPR ranged from 25.2%-67.0%. By years 4 and 5 (months 37 to 60) of sustained IRS these metrics had decreased to 30-90 and 8.5%-26.3%, respectively. However, in year 6 and the first half of year 7 (months 61 to 78) of sustained IRS, average monthly cases adjusted for testing increased to a range of 129-544 and TPR ranged from 18.7%-49.0%. **Figure 3.2** shows plots of laboratory-confirmed malaria cases and vector control interventions over time across the 5 sites. Each of these sites demonstrate similar patterns of a decline in malaria cases after the initiation of IRS with seasonal peaks during the first three years of IRS (through 2017), a substantial decline in burden in years four and five of sustained IRS (through 2019), and an increase in burden in years 6 and 7 of sustained IRS (2020-2021) equal to or higher than burden in the baseline period before IRS was implemented.

Monthly adjusted IRRs and 95% confidence intervals (CI) for the 5 sites combined are presented in **Figure 3.3**. These results show there was an initial 52% reduction in malaria burden in months 1 through 36 of sustained IRS (adjusted IRR = 0.48, 95% CI 0.40-0.58), followed by an 84% reduction in burden in months 37 through 60 of sustained IRS (adjusted IRR = 0.16, 95% CI 0.13-0.20). In months 61 through 72, malaria burden was 43% lower than the baseline period before IRS was implemented (adjusted IRR = 0.57, 95% CI 0.45-0.72). During months 73 through 78 after the initiation of IRS, malaria burden was 25% higher than the pre-IRS period, although we could not rule out a null or negative association (adjusted IRR = 1.25, 95% CI 0.93-1.69). These results were consistent when including only laboratory-confirmed cases unadjusted for testing rate as the model outcome (**Appendix Figure 3.1**) and when repeating the analysis leaving out the 2 sites that halted IRS campaigns in 2021 (Orum and Alebtong) (**Appendix Figure 3.2**).

Study Objective 2

Across the 15 sites over a 19 month period (January 2020 through July 2021) included in the analysis for Objective 2, 1,368,587 outpatient visits were recorded (**Table 3.2**). From January 2020 through December 2020, average monthly cases at IRS sites ranged from 64-594 and TPR ranged from 10.9%-51.0%. From January 2021 through July 2021, these figures increased to 235-745 and 27.2%-61.3%, respectively. Average monthly cases increased in 4 of the 5 sites from January 2020 through December 2020 to January 2021 through July 2021, with the exception of Dokolo (the first site to switch to IRS with a clothianidin-based formulation in 2019), which already experienced a large increase in monthly malaria cases by January 2020.

In sites that have not received IRS recently, average monthly cases from January 2020 through December 2020 ranged from 518-1,068 and TPR from 47.5%-71.1%. These figures decreased to 216-775 and 29.5%-51.5%, respectively, from January 2021 through July 2021. **Figure 3.4** shows plots of laboratory-confirmed malaria cases and the timing of the recent LLIN distribution across the 10 non-IRS sites from January 2020 through July 2021. These figures indicate a substantial increase in cases the first year of observation for some sites, but a general downward trend in cases across the 10 sites over the 19 month study period for Objective 2.

Figure 3.5 shows the mean number of cases across the 5 IRS sites and the 10 sites that have not received IRS recently from January 2020 to July 2021 (corresponding to months 60 through 78 of IRS for the 5 sites where IRS was initiated and sustained). This figure shows an increase in cases at IRS sites, particularly in the latter half of the observation window, while cases at non-IRS sites trended downward over the same time period. **Figure 3.5** also shows the adjusted IRR comparing cases at IRS sites to sites that have not received IRS recently. These findings indicate that from January 2020 to November 2020, cases were significantly lower in IRS sites compared to non-IRS sites. From December 2020 onward, the IRR crossed 1, indicating that cases at IRS sites were higher than non-IRS sites, although we could not rule out a null or negative association in these months. These results show that cases were 69% lower in IRS sites than non-IRS sites from January 2020 through December 2020 (adjusted IRR = 0.31, 95% CI 0.19-0.51) and 20% higher from January through July 2021 (adjusted IRR = 1.20, 95% CI 0.72-2·00). Results were consistent when including only laboratory-confirmed cases unadjusted for testing as the outcome (**Appendix Figure 3.3**).

Discussion

We utilized enhanced health facility surveillance data from 5 sites in East and Northeast Uganda that have undergone sustained IRS since 2014 to evaluate the impact of repeated IRS campaigns in their 6th and 7th years. Our findings point to a resurgence in the burden of malaria at these 5 health facilities, despite sustained IRS and repeated LLIN universal coverage campaigns conducted every 3 years. In the final six months of observation (months 61-78 of sustained IRS), malaria burden reached similar levels, and in some instances higher levels, from the period before IRS was initiated in late 2014. We did not observe corresponding increases in burden at 10 surveillance sites in neighboring non-IRS districts that, unlike IRS districts, received "next generation" LLINs over the study period. These findings suggest that in the setting of universal coverage with conventional pyrethroid-only LLINs, the marked benefit of adding sustained IRS over the first five years had been lost over the subsequent 18 months.

This study underscores the importance of high quality routine surveillance to monitor the impact of population level malaria control interventions using clinically relevant indicators such as symptomatic cases diagnosed at health facilities. The assessment of vector control interventions often focuses on entomologic outcomes such as mosquito mortality in controlled settings. This is understandable, given that measuring the impact of control interventions on clinical burden in "real world" settings is difficult. Nevertheless, the findings from this analysis underscore the need for robust epidemiologic surveillance systems to document the impact of vector control interventions on population health as they are applied.

Routine surveillance in areas undergoing IRS is particularly necessary because published studies from controlled trials on the added value of IRS in areas with high LLIN coverage has produced mixed results. A recent Cochrane review reported that adding IRS using a "pyrethroid-like" insecticide to LLINs did not provide any benefits, while adding IRS with a "non-pyrethroid-like" insecticide produced mixed results (67). It is of note that none of the trials that evaluated the impact of adding IRS with a "non-pyrethroid-like" insecticide assessed outcomes beyond two years. More recently, observational studies evaluating the effectiveness of pirimiphos-methyl (Actellic 300CS®) in "real world" settings have documented impressive impacts of IRS in Mali (70, 71), Ghana (72), Zambia (73), Kenya (74), and Uganda (50). This analysis contributes to observational data on the impacts of sustained IRS beyond 6 years, in the context of the COVID-19 pandemic and a switch to products containing the active ingredient clothianidin.

There are several potential factors that may be driving the increase in malaria burden in districts receiving IRS. First, the timing of the increase corresponds to a shift in active ingredient from pirimiphos-methyl to clothianidin-based formulations (primarily Fludora® Fusion, a combination of clothianidin and deltamethrin). This change may have led to a loss of the additive effect of dual interventions (combining pirimiphos-methyl to pyrethroid LLINs), which would be particularly detrimental as wide-spread pyrethroid resistance has been described in Uganda (75-77). Given that IRS districts received conventional pyrethroid LLINs in the 2020-2021 UCC campaign, pyrethroid resistance may also explain why burden increased at IRS sites despite the campaign. Conversely, the 10 sites in neighboring districts where increases in burden were not observed received "next generation" nets designed for areas with wide-spread pyrethroid resistance. Of note, the one site (Dokolo) that received a single round of IRS with clothianidin-

based Sumishield® 50WG in 2019 (before the shift to Fludora® Fusion WP-SB across all sites in 2020) experienced an increase in burden immediately following the round of Sumishield® 50WG. Increases were not documented at other sites until the initiation of Fludora® Fusion WP-SB in 2020. This is added evidence for the change in active ingredient contributing to the observed resurgence of malaria. To date, studies on the effectiveness of clothianidin alone (Sumishield®) (78-82) and clothianidin with deltamethrin (Fludora® Fusion WP-SB) (78, 83-85) are limited to susceptibility studies focused on entomological outcomes, both in lab and in experimental huts. These studies document that clothianidin-based products succeed at killing mosquitoes, but none have evaluated clinically relevant outcomes in "real world" settings.

A second potential contributor to the observed resurgence of malaria at sites receiving IRS is the COVID-19 pandemic. An important concern has been the potential for delayed or inadequate implementation of vector control measures due to the pandemic (86, 87). In Uganda, the UCC LLIN distribution was delayed by 5 months but successfully distributed over 28 million nets, achieving over 90% coverage. Given the delay in the UCC was country-wide, we do not believe an increase in burden resulting from delayed net distribution would be observed strictly in IRS sites as was the case in this study. The implementation of IRS campaigns did not appear impacted by the COVID-19 pandemic; annual campaigns in 2020 and 2021 were not delayed and coverage remained high (>90%, see **Appendix Table 3.1**). We cannot rule out the potential for undocumented differences in implementation (for example, if spray operators spent less time in homes due to fear of acquiring COVID-19) that may have contributed to the observed resurgence. The pandemic may also have impacted patient behavior; for example, patients may have delayed seeking care for malarial illness which could have led to increased transmission.

However, because sites that have not recently received IRS did not observe an increase in transmission, this explanation is less tenable.

Another potential explanation is a shift in mosquito species composition or mosquito behavior to outdoor biting, circumventing vector control interventions that target indoor biting mosquitoes (88). This, however, would be unlikely to have occurred rapidly and simultaneously at all IRS sites at a pace that would explain the resurgence observed in this study. In addition, this would not explain the observation that the resurgence was observed only in the IRS sites and not in the non-IRS sites that only received LLINs, as a shift to outdoor biting would have a negative impact on both IRS and LLINs. Similarly, a shift in the predominant species from *Anopheles gambiae* and *Anopheles funestus* to *Anopheles arabiensis* may have led to a change from predominately indoor to outdoor biting (89). Recent data demonstrate that *Anopheles gambiae* and *Anopheles funestus* remain the primary vectors in Uganda (77), but other work has documented the near collapse of *Anopheles gambiae* and *Anopheles funestus* in areas with an LLIN distribution and repeated IRS campaigns (89).

This study is not without limitations. First, we used an observational study design, with measures of impact based on comparisons made before-and-after the implementation of IRS and comparisons of IRS and non-IRS districts. While cluster randomized controlled trials remain the gold standard design for estimating the impact of IRS, withholding IRS may be unethical, given what is known about its beneficial impacts, particularly in Uganda (50). Similarly, comparisons of IRS sites and sites that have not recently received IRS are strictly descriptive, given that districts receiving IRS and not receiving IRS are not exchangeable. Second, while we

hypothesize potential mechanisms that may explain the observed resurgence in malaria burden in IRS sites, we cannot rule potential secular trends or other unmeasured contributing factors. However, overall secular trends are an unlikely cause given the contemporaneous decline in malaria burden at nearby non-IRS sites. Third, the outcome for this analysis is limited to case counts of laboratory-confirmed malaria captured at health facilities. We do not have additional data on other metrics of transmission intensity, including entomologic measures, nor on malaria mortality.

Despite these limitations, this analysis has important policy implications. First, the Ministry of Health should be prepared to make timely changes in malaria control interventions based on on-going surveillance. For example, in IRS districts, policy makers may consider prioritizing the use of newer generation LLINs containing PBO which have been shown to be more effective than traditional pyrethroid treated LLINs in Uganda (90). Future changes to the IRS active ingredient should be made based on on-going surveillance and should be in line with Uganda's resistance management strategy. Consideration should also be made to key logistical factors including cost, procurement, and community acceptability. The unprecedented increase in malaria burden in areas where incidence had declined by 85% underscores the need to remain vigilant. Indeed, two of the five IRS districts included in this analysis stopped receiving IRS altogether in 2021, underscoring the challenge of maintaining gains in the face of inadequate resources and the need for rational exit strategies when IRS cannot be sustained. Finally, maintaining high quality, continuous surveillance systems to assess the impact of population level malaria control interventions remains essential in order to generate timely, actionable data.

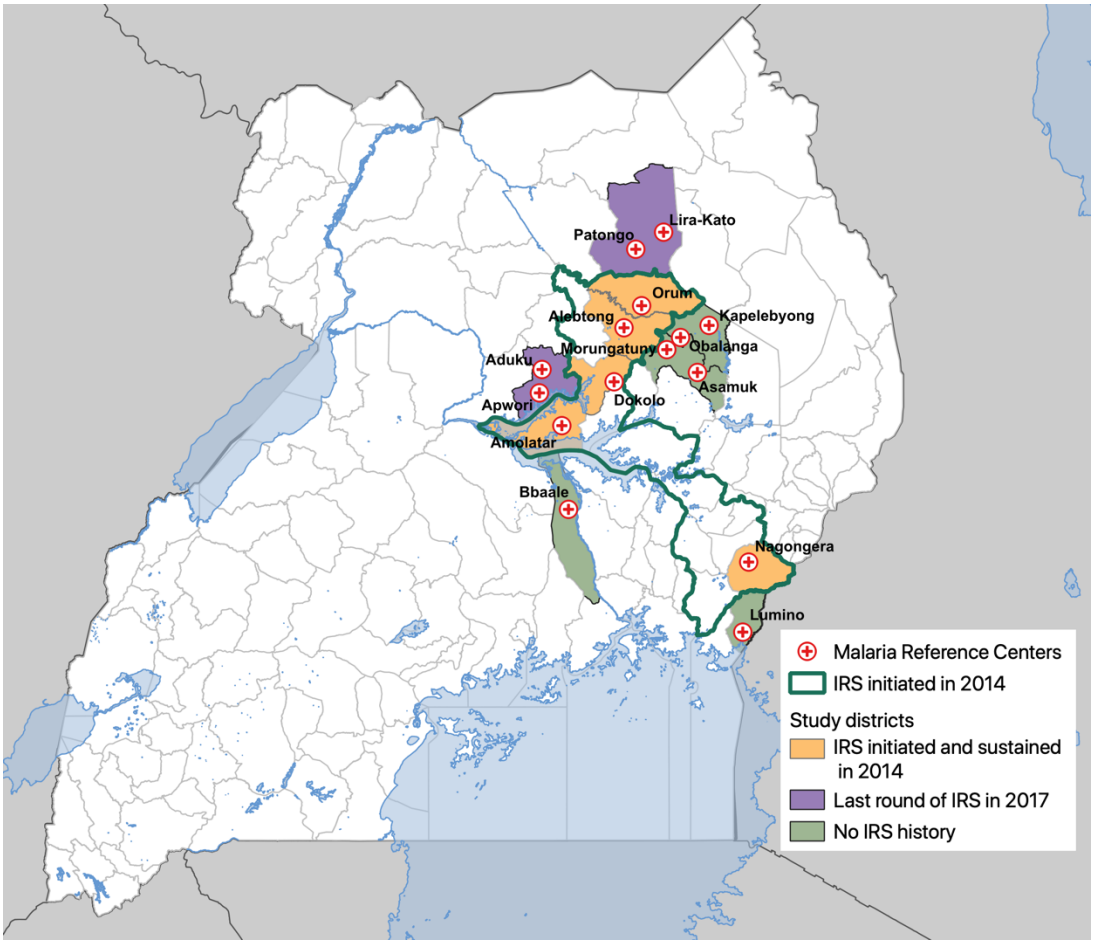

Figure 3.1. Map of Uganda showing study sites.

Table 3.1. Summary statistics from health-facility based surveillance sites for study objective 3

MRC (District)	Time period	Total outpatient visits, n	Suspected malaria cases, n (% of outpatient visits)	Tested for malaria, n (% of suspected malaria cases)	RDT performed (versus microscopy), n (% of tested)	Confirmed malaria cases, n (% of tested [TPR])	Confirmed malaria cases adjusted for testing	Mean monthly malaria cases adjusted for testing
Nagongera HCIV (Tororo)	Baseline (12 months pre-IRS)	20,828	13,251 (63.6)	13,096 (98.8)	760 (5.8)	3,298 (25.2)	3,337	278
	Months 1 through 36 of IRS	63,289	23,315 (38.4)	24,084 (99.0)	9,615 (40.0)	4,004 (16.6)	4,042	112
	Months 37 through 60 of IRS	35,745	12,616 (35.2)	12,608 (99.9)	3,798 (30.1)	1,067 (8.5)	1,067	30
	Months 61 through 78 of IRS	32,158	12,449 (38.7)	12,445 (99.9)	10,452 (84.0)	2,328 (18.7)	2,328	129
Amolatar HCIV (Amolatar)	Baseline (12 months pre-IRS)	19,552	8,547 (43.7)	6,512 (76.2)	5,923 (91.0)	3,701 (56.8)	4,845	404
	Months 1 through 36 of IRS	55,570	18,118 (32.6)	15,082 (83.2)	13,440 (89.1)	3,924 (26.0)	4,956	138
	Months 37 through 60 of IRS	35,231	7,038 (20.0)	7,034 (99.9)	6,279 (89.3)	908 (12.9)	1,088	30
	Months 61 through 78 of IRS	29,133	10,936 (37.5)	10,906 (99.7)	8,967 (82.2)	5,848 (45.2)	5,866	326
Dokolo HCIV (Dokolo)	Baseline (12 months pre-IRS)	25,570	12,854 (50.3)	8,875 (69.0)	8,212 (92.5)	5,211 (58.7)	7,889	657
	Months 1 through 36 of IRS	78,969	30,846 (39.1)	29,476 (95.6)	27006 (91.6)	7,734 (26.2)	8,266	230
	Months 37 through 60 of IRS	52,550	16,361 (31.1)	16,273 (99.5)	15,997 (98.3)	2,524 (15.6)	3,243	90
	Months 61 through 78 of IRS	47,484	20,253 (42.7)	20,215 (99.8)	17,975 (88.9)	9,766 (48.3)	9,784	544
Orum HCIV (Otuke)	Baseline (11 months pre-IRS)	16,120	9,324 (57.8)	8,929 (95.8)	3,990 (44.7)	5,974 (66.9)	6,236	566
	Months 1 through 36 of IRS	42632	26,642 (62.5)	25,583 (96.0)	11008 (43.0)	13,619 (53.2)	14,207	394
	Months 37 through 60 of IRS	23,424	11,064 (47.2)	11,064 (100.0)	8,717 (78.9)	2,911 (26.3)	3,072	85
	Months 61 through 78 of IRS	17,374	11,015 (63.4)	11,015 (100.0)	8,287 (75.2)	5,393 (49.0)	5,393	300
Alebtong HCIV (Alebtong)	Baseline (8 months pre-IRS)	15,359	6,694 (43.6)	4,789 (71.5)	4,620 (96.5)	3,209 (67.0)	4,317	540
	Months 1 through 36 of IRS	62,161	30,226 (48.6)	25,863 (85.6)	22,373 (86.5)	10,452 (40.4)	12,251	340
	Months 37 through 60 of IRS	33,201	11,091 (33.4)	10,810 (97.5)	10,399 (96.2)	1,638 (15.1)	1,745	48
	Months 61 through 78 of IRS	32,782	17,434 (53.2)	17,434 (100.0)	14,251 (81.7)	7,884 (45.2)	7,884	438

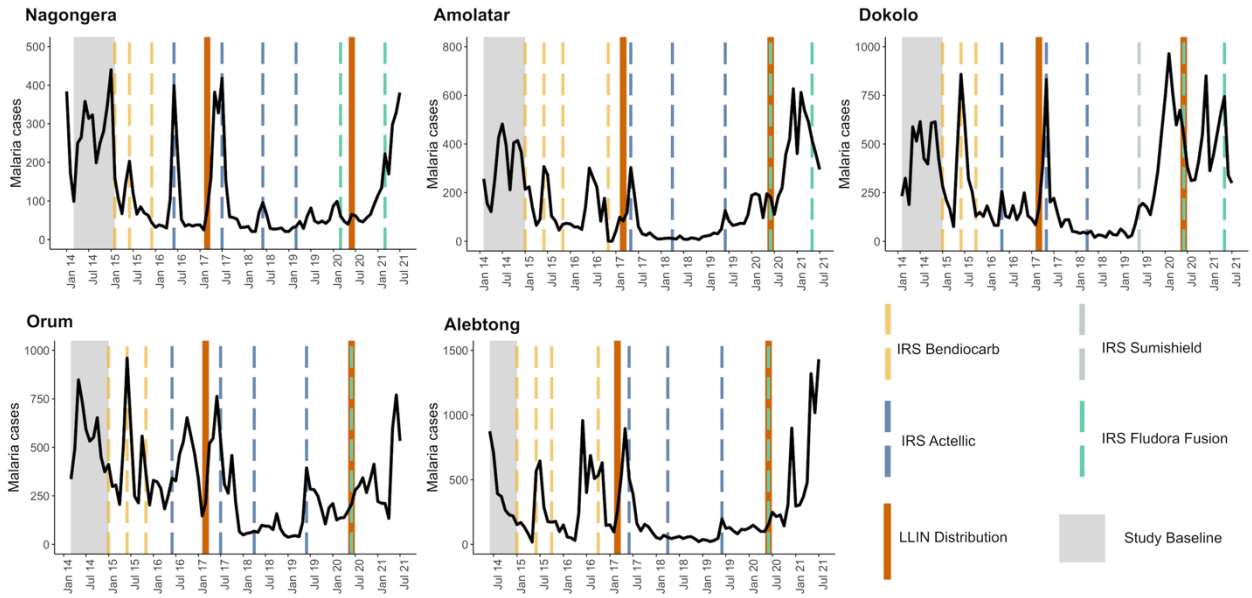

Figure 3.2. Malaria case counts and vector control interventions over time at 5 IRS sites. The study baseline period (pre-IRS) is indicated in grey.

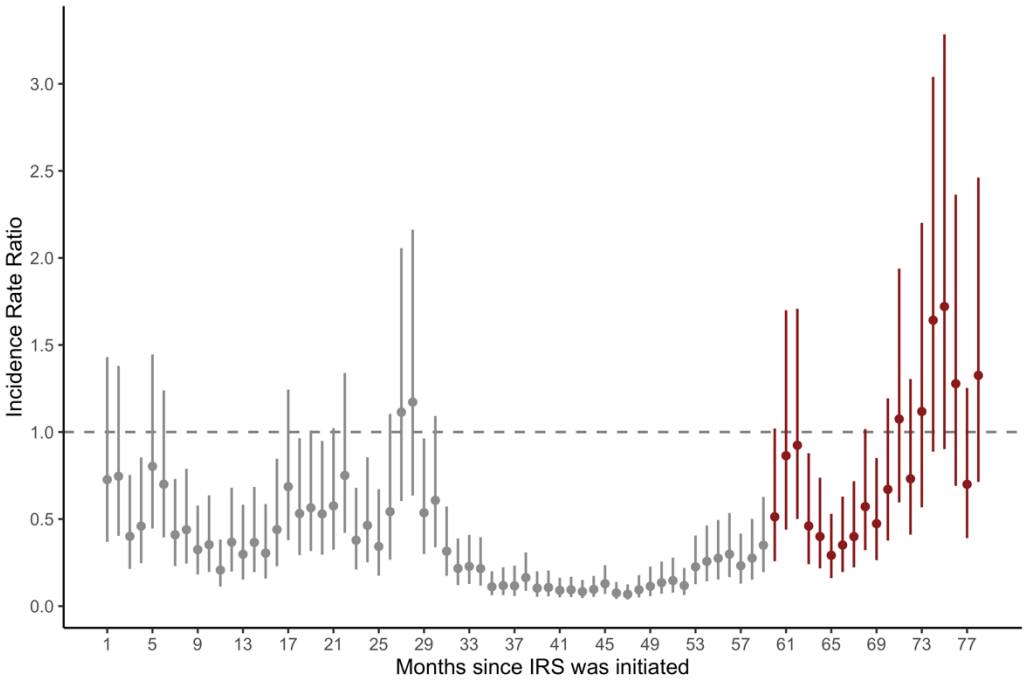

Figure 3.3. Adjusted IRR from multilevel negative binomial model comparing the period after IRS was initiated to the period before IRS was initiated. Vertical bars represent the 95% CI around adjusted IRR. Effect estimates in grey are published previously.

Table 3.2. Summary statistics from health-facility based surveillance sites for study objective 2

MRC (District)	Time period	Total outpatient visits, n	Suspected malaria cases, n (% of outpatient visits)	Tested for malaria, n (% of suspected malaria cases)	RDT performed (versus microscopy), n (% of tested)	Confirmed malaria cases, n (% of tested [TPR])	Confirmed malaria cases adjusted for testing	Mean monthly malaria cases adjusted for testing
				IRS SITES				
Nagongera HCIV (Tororo)	January 2020-December 2020	20,079	7,033 (35.0)	7,031 (99.9)	5,706 (81.2)	767 (10.9)	767	64
	January 2021-July 2021	14,101	6,039 (42.8)	6,037 (99.9)	5,030 (83.3)	1,648 (27.2)	1,648	235
Amolatar HCIV (Amolatar)	January 2020-December 2020	18,995	6,360 (33.5)	6,349 (99.8)	5,198 (81.9)	2,965 (46.7)	2,969	247
	January 2021-July 2021	11,851	5,036 (42.5)	5,015 (99.5)	4,206 (83.9)	3,072 (61.3)	3,087	441
Dokolo HCIV (Dokolo)	January 2020-December 2020	32,042	13,984 (43.6)	13,947 (99.7)	12,842 (92.1)	7,110 (51.0)	7,130	594
	January 2021-July 2021	18,245	7,588 (41.6)	7,577 (99.9)	6,421 (84.7)	3,398 (44.8)	3,402	486
Orum HCIV (Otuke)	January 2020-December 2020	11,161	6,807 (61.0)	6,807 (100.0)	5,672 (83.3)	2,925 (43.0)	2,925	244
	January 2021-July 2021	7,237	4,772 (65.9)	4,772 (100.0)	3,126 (65.5)	2,678 (56.1)	2,678	383
Alebtong HCIV (Alebtong)	January 2020-December 2020	19,027	8,877 (46.7)	8,877 (100.0)	7,763 (87.5)	2,797 (31.5)	2,797	233
	January 2021-July 2021	14,932	9,069 (60.7)	9,069 (100.0)	6,981 (77.0)	5,214 (57.4)	5,214	745
				NON-IRS SITES				
Aduku HCIV (Kwania)	January 2020-December 2020	26,537	19,136 (72.1)	19,133 (99.9)	12,770 (66.7)	12,818 (67.0)	12,821	1,068
	January 2021-July 2021	16,004	10,542 (65.9)	10,535 (99.9)	6,298 (59.8)	5,422 (51.5)	5,426	775
Patongo HCIII (Agago)	January 2020-December 2020	21,138	18,076 (85.6)	18,071 (99.9)	17,417 (96.4)	11,911 (65.9)	11,914	993
	January 2021-July 2021	8,327	6,564 (78.9)	6,564 (100.0)	5,835 (88.9)	2,613 (39.8)	2,613	373
Bbaale HCIV (Kayunga)	January 2020-December 2020	25,382	15,691 (61.8)	15,591 (99.4)	11,856 (76.0)	7,401 (47.5)	7,450	621
	January 2021-July 2021	11,476	6,664 (58.1)	6,640 (99.6)	5,004 (75.4)	2,202 (33.1)	2,210	316
Lumino HCIII (Busia)	January 2020-December 2020	21,885	17,783 (81.2)	17,783 (100.0)	16,094 (90.5)	10,409 (58.5)	10,409	867
	January 2021-July 2021	11,034	8,551 (77.4)	8,551 (100.0)	7,189 (84.1)	4,212 (49.3)	4,212	602
Apwori HCIII (Kwania)	January 2020-December 2020	14,759	13,783 (93.4)	13,781 (99.9)	12,189 (88.5)	9,164 (66.5)	9,166	764
	January 2021-July 2021	6,843	5,921 (86.5)	5,921 (100.0)	5,877 (99.3)	2,061 (34.8)	2,061	294
Lira-Kato HCIII (Agago)	January 2020-December 2020	20,059	17,825 (88.9)	17,814 (99.9)	17,801 (99.9)	12,670 (71.1)	12,679	1057
	January 2021-July 2021	8,753	6,796 (77.6)	6,795 (99.9)	5,921 (87.1)	3,491 (51.4)	3,491	499
Morungatuny HCIII (Amuria)	January 2020-December 2020	15,053	13,964 (92.7)	13,964(100.0)	13,940 (99.8)	7,698 (55.1)	7,698	642
	January 2021-July 2021	7,427	7,288 (98.1)	7,288(100.0)	7,287 (99.9)	2,162 (29.7)	2,162	309
Asamuk HCIII (Amuria)	January 2020-December 2020	20,504	18,065 (88.1)	18,045 (99.9)	17,633 (97.7)	10,728 (59.5)	10,742	895
	January 2021-July 2021	12,505	11,129 (89.0)	11,129(100.0)	11,098 (99.7)	3,804 (34.8)	3,804	543
Kapelebyong HCIV (Kapelebyong)	January 2020-December 2020	16,975	10,720 (63.2)	10,711 (99.9)	10,652 (99.5)	6,215 (58.0)	6,219	518
	January 2021-July 2021	10,287	5,111 (49.7)	5,111(100.0)	5,108 (99.9)	1,510 (29.5)	1,510	216

Obalanga HCIII (Kapelebyong)	January 2020-December 2020	17,438	15,855 (90.9)	15,852 (99.9)	12,833 (81.0)	9,917 (62.6)	9,919	827
	January 2021-July 2021	8,419	7,863 (93.4)	7,863(100.0)	6,963 (88.6)	3,286 (41.7)	3,286	469

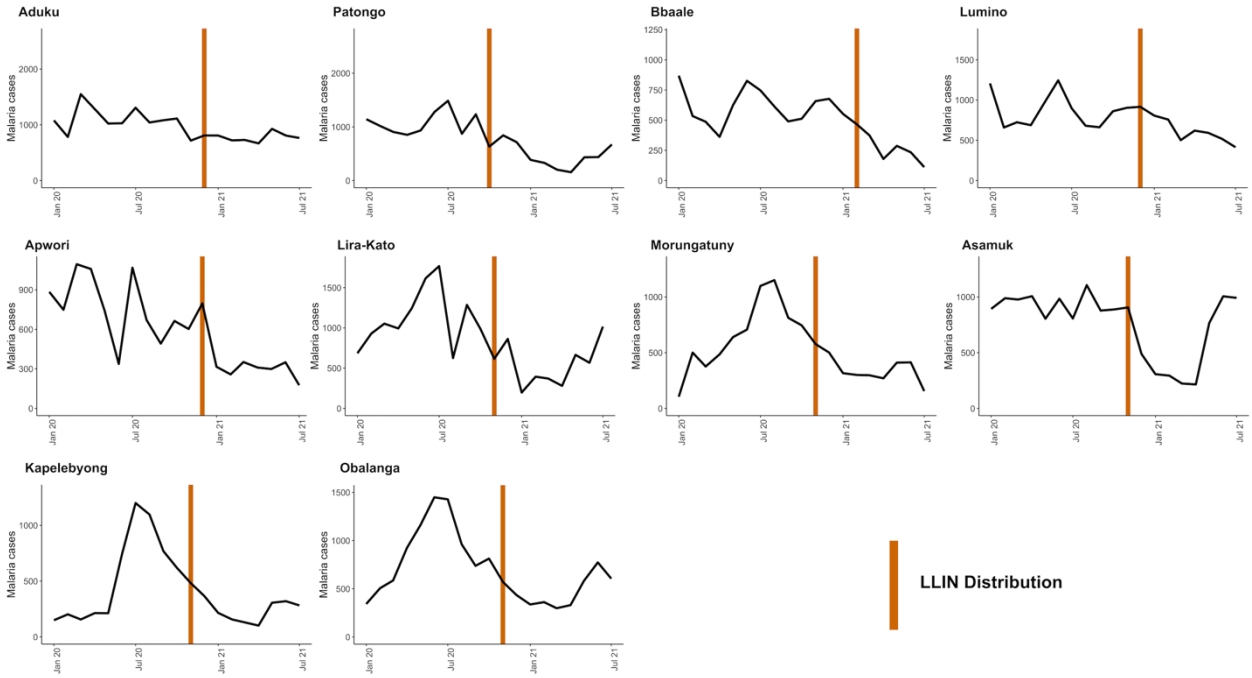

Figure 3.4. Malaria case counts and vector control interventions over time at 10 sites that have not received IRS recently.

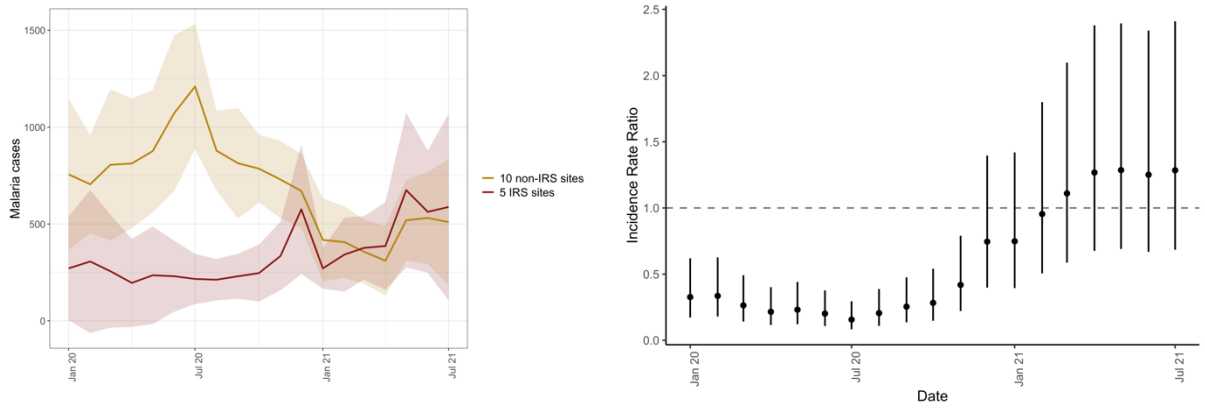

Figure 3.5. Mean case counts in 5 IRS sites and 5 non-IRS sites from January 2020 through July 2021 (left) and adjusted IRR comparing IRS sites to non-IRS sites over the study period. Shaded areas represent standard deviations. Vertical bars represent the 95% CI around adjusted IRR.

Chapter 3 Appendix

Appendix Table 3.1. Timing and formulation IRS campaigns.

MRC	District	Details of IRS campaign	1st round (Coverage)	2nd round (Coverage)	3rd round (Coverage)	4th round (Coverage)	5th round (Coverage)	6th round (Coverage)	7th round (Coverage)	8th round (Coverage)	9th round (Coverage)
Nagongera HCIV	Tororo	Date	08-Dec-14 to 19-Feb-15	08-Jun-15 to 12-Jul-15	02-Nov-15 to 12-Dec-15	12-Jun-16 to 9-Jul-16	17-July-17 to 19-Aug-17	11-Jun-18 to 27-7-18	18-Mar-19 to 15-Apr-19	2-Mar-20 to 28-Mar-2020	1-Mar-20 to 26-Mar-2021
		Formulation	Bendiocarb	Bendiocarb	Bendiocarb	Actelic	Actellic	Actellic	Actellic	Fludora Fusion WP-SB*	Fludora Fusion WP-SB
		Coverage	Not available	(94.60%)	(96.30%)	(93.0%)	(94.90%)	(95.80%)	(92.10%)	(93.20%)	(99.4%)
Amolatar HCIV	Amolatar	Date	08-Dec-14 to 19-Feb-15	08-Jun-15 to 12-Jul-15	12-Oct-15 to 07-Nov-15	24-Oct-16 to 19-Nov-16	2-May-17 to 6-June-17	9-Apr-18 to 12-May-18	27-May-19 to 27-June-19	25-May-2020 to 20-Jun-2020	26 April to 20 May 2021
		Formulation	Bendiocarb	Bendiocarb	Bendiocarb	Bendiocarb	Actellic	Actellic	Actellic	Fludora Fusion WP-SB†	Fludora Fusion WP-SB
		Coverage	Not available	(96.10%)	(91.40%)	(94.1%)	(95.80%)	(96.10%)	(94.20%)	(96.20%)	(91.5%)
Dokolo HCIV	Dokolo	Date	08-Dec-14 to 19-Feb-15	08-Jun-15 to 12-Jul-15	12-Oct-15 to 07-Nov-15	18-Apr-16 to 9-Jul-16	2-May-17 to 6-June-17	9-Apr-18 to 12-May-18	27-May-19 to 27-June-19	25-May-2020 to 20-Jun-2020	26 April to 25 May 2021
		Formulation	Bendiocarb	Bendiocarb	Bendiocarb	Actellic	Actellic	Actellic	Sumishield 50W	Fludora Fusion WP-SB†	Fludora Fusion WP-SB
		Coverage	Not available	(88.70%)	(92.10%)	(94.80%)	(97.60%)	(94.30%)	(95.20%)	(94.60%)	(91.0%)
Orum HCIV	Otuke	Date	08-Dec-14 to 19-Feb-15	08-Jun-15 to 12-Jul-15	02-Nov-15 to 12-Dec-15	18-Apr-16 to 9-Jul-16	17-July-17 to 19-Aug-17	11-Jun-18 to 27-7-18	27-May-19 to 27-June-19	25-May-2020 to 20-Jun-2020	
		Formulation	Bendiocarb	Bendiocarb	Bendiocarb	Actellic	Actellic	Actellic	Actellic	Fludora Fusion WP-SB†	
		Coverage	Not available	(96.60%)	(94.80%)	(97.60%)	(96.70%)	(98.40%)	(98.80%)	(96.50%)	
Alebtong HCIV	Alebtong	Date	08-Dec-14 to 19-Feb-15	08-Jun-15 to 12-Jul-15	12-Oct-15 to 07-Nov-15	24-Oct-16 to 19-Nov-16	2-May-17 to 6-June-17	9-Apr-18 to 12-May-18	27-May-19 to 27-June-19	25-May-2020 to 20-Jun-2020	
		Formulation	Bendiocarb	Bendiocarb	Bendiocarb	Bendiocarb	Actellic	Actellic	Actellic	Fludora Fusion WP-SB†	
		Coverage	Not available	(96.90%)	(95.40%)	(97.50%)	(98.30%)	(90.90%)	(95.00%)	(95.50%)	

*2% of households received Actellic

†2% of households received Sumishield 50W

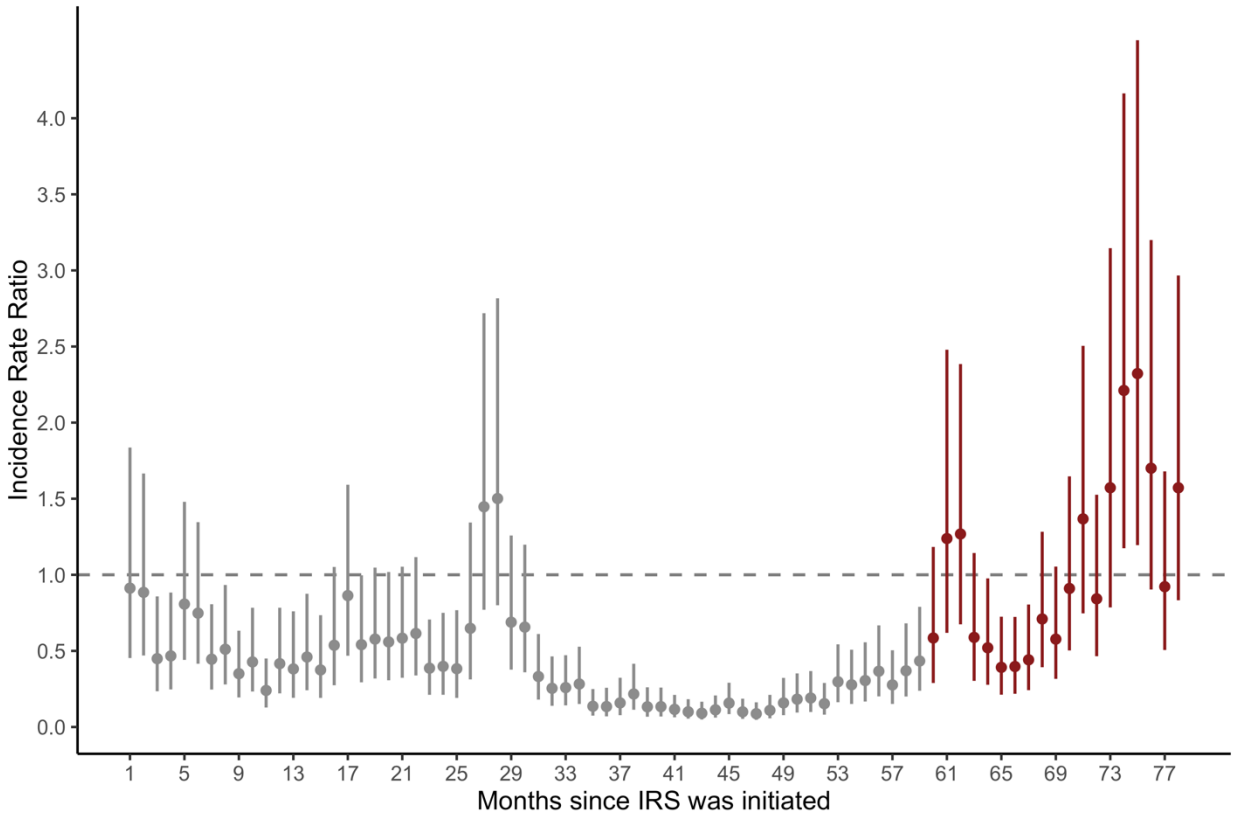

Appendix Figure 3.1. Adjusted IRR from multilevel negative binomial model comparing the period after IRS was initiated to the period before IRS was initiated with unadjusted case counts as model outcome. Vertical bars represent the 95% CI around adjusted IRR. Effect estimates in grey are published previously.

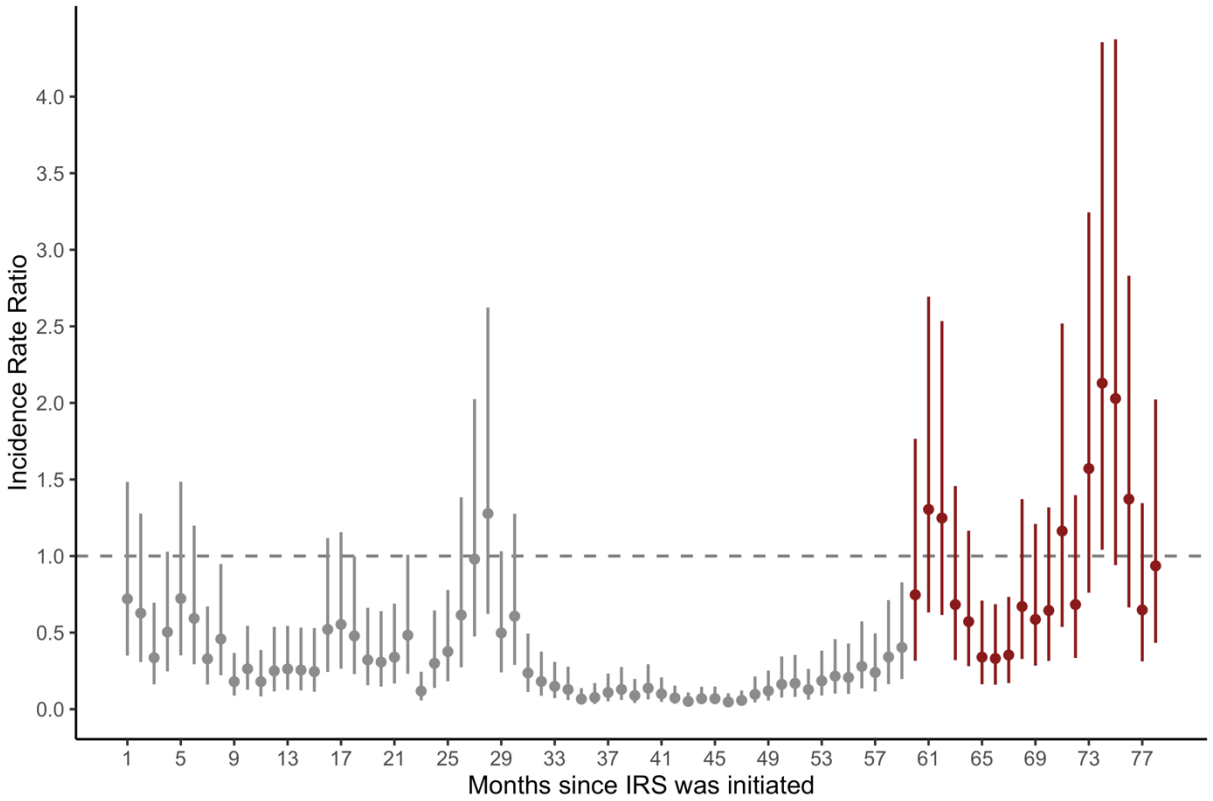

Appendix Figure 3.2. Adjusted IRR from multilevel negative binomial model comparing the period after IRS was initiated to the period before IRS was initiated leaving out 2 sites that stopped IRS in 2021 (Orum and Alebtong). Vertical bars represent the 95% CI around adjusted IRR. Effect estimates in grey are published previously.

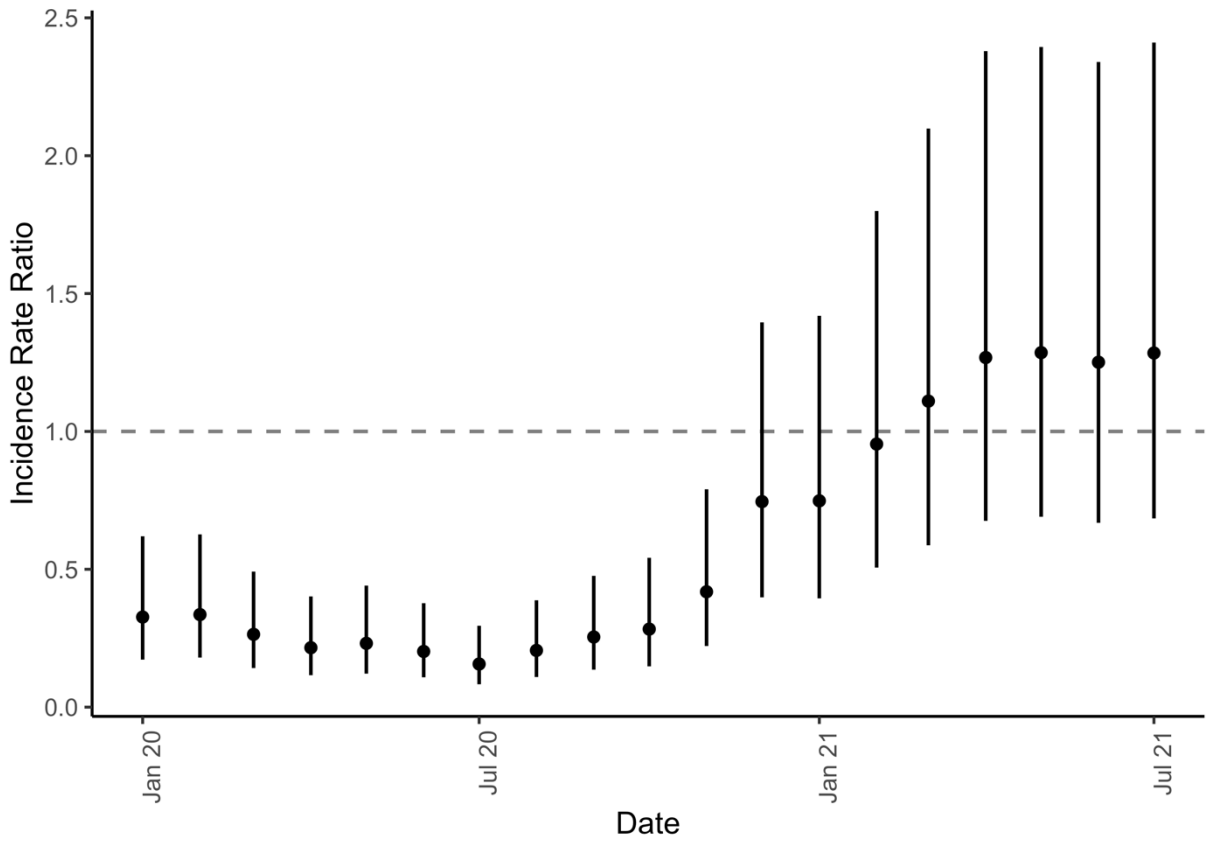

Appendix Figure 3.3. Adjusted IRR comparing IRS sites to non-IRS sites over the study period with unadjusted case counts as model outcome. Vertical bars represent the 95% CI around adjusted IRR.

References

1. World Malaria Report 2018. Geneva: World Health Organization; 2018.

2. Breman JG, Holloway CN. Malaria surveillance counts. Am J Trop Med Hyg. 2007;77(6 Suppl):36-47.

3. Malaria surveillance, monitoring & evaluation: a reference manual. Geneva: World Health Organization; 2018.

4. Pinchoff J, Chaponda M, Shields T, Lupiya J, Kobayashi T, Mulenga M, et al. Predictive Malaria Risk and Uncertainty Mapping in Nchelenge District, Zambia: Evidence of Widespread, Persistent Risk and Implications for Targeted Interventions. Am J Trop Med Hyg. 2015;93(6):1260-7.

5. Carter R, Mendis KN, Roberts D. Spatial targeting of interventions against malaria. Bull World Health Organ. 2000;78(12):1401-11.

6. Global technical strategy for malaria 2016-2030. Geneva: World Health Organization; 2015.

7. Disease surveillance for malaria control: an operational manual. Geneva: World Health Organization; 2012.

8. Cameron E, Battle KE, Bhatt S, Weiss DJ, Bisanzio D, Mappin B, et al. Defining the relationship between infection prevalence and clinical incidence of Plasmodium falciparum malaria. Nat Commun. 2015;6:8170.

9. Bhatt S, Weiss DJ, Cameron E, Bisanzio D, Mappin B, Dalrymple U, et al. The effect of malaria control on Plasmodium falciparum in Africa between 2000 and 2015. Nature. 2015;526(7572):207-11.

10. Ohrt C, Roberts KW, Sturrock HJW, Wegbreit J, Lee BY, Gosling RD. Information systems to support surveillance for malaria elimination. Am J Trop Med Hyg. 2015;93(1):145-52.

11. Howes RE, Mioramalala SA, Ramiranirina B, Franchard T, Rakotorahalahy AJ, Bisanzio D, et al. Contemporary epidemiological overview of malaria in Madagascar: operational utility of reported routine case data for malaria control planning. Malar J. 2016;15(1):502.

12. Rowe AK. Assessing the Health Impact of Malaria Control Interventions in the MDG/Sustainable Development Goal Era: A New Generation of Impact Evaluations. Am J Trop Med Hyg. 2017;97(3_Suppl):6-8.

13. Ashton RA, Bennett A, Yukich J, Bhattarai A, Keating J, Eisele TP. Methodological Considerations for Use of Routine Health Information System Data to Evaluate Malaria Program Impact in an Era of Declining Malaria Transmission. Am J Trop Med Hyg. 2017;97(3_Suppl):46-57.

14. Alonso P, Noor AM. The global fight against malaria is at crossroads. Lancet. 2017;390(10112):2532-4.

15. Alegana VA, Okiro EA, Snow RW. Routine data for malaria morbidity estimation in Africa: challenges and prospects. BMC Med. 2020;18(1):121.

16. Francis D, Gasasira A, Kigozi R, Kigozi S, Nasr S, Kamya MR, et al. Health facility-based malaria surveillance: the effects of age, area of residence and diagnostics on test positivity rates. Malar J. 2012;11:229.

17. Boyce RM, Reyes R, Matte M, Ntaro M, Mulogo E, Lin FC, et al. Practical Implications of the Non-Linear Relationship between the Test Positivity Rate and Malaria Incidence. PLoS One. 2016;11(3):e0152410.

18. Jensen TP, Bukirwa H, Njama-Meya D, Francis D, Kamya MR, Rosenthal PJ, et al. Use of the slide positivity rate to estimate changes in malaria incidence in a cohort of Ugandan children. Malar J. 2009;8:213.

19. Sturrock HJ, Cohen JM, Keil P, Tatem AJ, Le Menach A, Ntshalintshali NE, et al. Fine-scale malaria risk mapping from routine aggregated case data. Malar J. 2014;13:421.

20. Alegana VA, Wright JA, Pentrina U, Noor AM, Snow RW, Atkinson PM. Spatial modelling of healthcare utilisation for treatment of fever in Namibia. Int J Health Geogr. 2012;11:6.

21. Kamya MR, Arinaitwe E, Wanzira H, Katureebe A, Barusya C, Kigozi SP, et al. Malaria transmission, infection, and disease at three sites with varied transmission intensity in Uganda: implications for malaria control. Am J Trop Med Hyg. 2015;92(5):903-12.

22. Sserwanga A, Harris JC, Kigozi R, Menon M, Bukirwa H, Gasasira A, et al. Improved malaria case management through the implementation of a health facility-based sentinel site surveillance system in Uganda. PLoS One. 2011;6(1):e16316.

23. Weiss DJ, Nelson A, Gibson HS, Temperley W, Peedell S, Lieber A, et al. A global map of travel time to cities to assess inequalities in accessibility in 2015. Nature. 2018;553(7688):333-6.

24. Pfeffer DA, Lucas TCD, May D, Harris J, Rozier J, Twohig KA, et al. MalariaAtlas: an R interface to global malariometric data hosted by the Malaria Atlas Project. Malar J. 2018;17(1):352.

25. Hastie T, Tibshirani R. Generalized additive models for medical research. Stat Methods Med Res. 1995;4(3):187-96.

26. Facebook Connectivity Lab and Center for International Earth Science Information Network - CIESIN - Columbia University. High Resolution Settlement Layer (HRSL): Source imagery for HRSL © 2016 DigitalGlobe; 2016 [

27. World Bank Open Data: World Bank; 2020 [Available from: https://data.worldbank.org/.

28. Kigozi SP, Pindolia DK, Smith DL, Arinaitwe E, Katureebe A, Kilama M, et al. Associations between urbanicity and malaria at local scales in Uganda. Malar J. 2015;14:374.

29. Kigozi SP, Giorgi E, Mpimbaza A, Kigozi RN, Bousema T, Arinaitwe E, et al. Practical Implications of a Relationship between Health Management Information System and Community Cohort-Based Malaria Incidence Rates. Am J Trop Med Hyg. 2020;103:404-14.

30. Ceesay SJ, Casals-Pascual C, Erskine J, Anya SE, Duah NO, Fulford AJ, et al. Changes in malaria indices between 1999 and 2007 in The Gambia: a retrospective analysis. Lancet. 2008;372(9649):1545-54.

31. O'Meara WP, Bejon P, Mwangi TW, Okiro EA, Peshu N, Snow RW, et al. Effect of a fall in malaria transmission on morbidity and mortality in Kilifi, Kenya. Lancet. 2008;372(9649):1555-62.

32. Birhanu Z, Abebe L, Sudhakar M, Dissanayake G, Yihdego YY, Alemayehu G, et al. Malaria Related Perceptions, Care Seeking after Onset of Fever and Anti-Malarial Drug Use in Malaria Endemic Settings of Southwest Ethiopia. PLoS One. 2016;11(8):e0160234.

33. Mota RE, Lara AM, Kunkwenzu ED, Lalloo DG. Health seeking behavior after fever onset in a malaria-endemic area of Malawi. Am J Trop Med Hyg. 2009;81(6):935-43.

34. Uganda Bureau of Statistics & Macro International Inc. Uganda Demographic and Health Survey 2011. Calverton, Maryland, USA; 2012.

35. Katureebe A, Zinszer K, Arinaitwe E, Rek J, Kakande E, Charland K, et al. Measures of Malaria Burden after Long-Lasting Insecticidal Net Distribution and Indoor Residual Spraying at Three Sites in Uganda: A Prospective Observational Study. PLoS Med. 2016;13(11):e1002167.

36. Alegana VA, Atkinson PM, Wright JA, Kamwi R, Uusiku P, Katokele S, et al. Estimation of malaria incidence in northern Namibia in 2009 using Bayesian conditional-autoregressive spatial-temporal models. Spat Spatiotemporal Epidemiol. 2013;7:25-36.

37. Alegana VA, Wright J, Pezzulo C, Tatem AJ, Atkinson PM. Treatment-seeking behaviour in low- and middle-income countries estimated using a Bayesian model. BMC Med Res Methodol. 2017;17(1):67.

38. Alegana VA, Atkinson PM, Lourenco C, Ruktanonchai NW, Bosco C, Erbach-Schoenberg EZ, et al. Advances in mapping malaria for elimination: fine resolution modelling of Plasmodium falciparum incidence. Sci Rep. 2016;6:29628.

39. Alegana VA, Khazenzi C, Akech SO, Snow RW. Estimating hospital catchments from in-patient admission records: a spatial statistical approach applied to malaria. Sci Rep. 2020;10(1):1324.

40. Uganda National Malaria Control Division (NMCD), Uganda Bureau of Statistics (UBOS), ICF. Uganda Malaria Indicator Survey 2018-19. Kampala, Uganda, and Rockville, Maryland, USA: NMCD, UBOS, and ICF; 2020.

41. World malaria report 2020: 20 years of global progress and challenges. Geneva: World Health Organization; 2020.

42. Odhiambo JN, Kalinda C, Macharia PM, Snow RW, Sartorius B. Spatial and spatio-temporal methods for mapping malaria risk: a systematic review. BMJ Glob Health. 2020;5(10).

43. Alegana VA, Wright J, Bosco C, Okiro EA, Atkinson PM, Snow RW, et al. Malaria prevalence metrics in low- and middle-income countries: an assessment of precision in nationally-representative surveys. Malar J. 2017;16(1):475.

44. Tusting LS, Bousema T, Smith DL, Drakeley C. Measuring changes in Plasmodium falciparum transmission: precision, accuracy and costs of metrics. Adv Parasitol. 2014;84:151-208.

45. O'Meara WP, Collins WE, McKenzie FE. Parasite prevalence: a static measure of dynamic infections. Am J Trop Med Hyg. 2007;77(2):246-9.

46. Thwing J, Camara A, Candrinho B, Zulliger R, Colborn J, Painter J, et al. A Robust Estimator of Malaria Incidence from Routine Health Facility Data. Am J Trop Med Hyg. 2020;102(4):811-20.

47. Macharia PM, Ray N, Giorgi E, Okiro EA, Snow RW. Defining service catchment areas in low-resource settings. BMJ Glob Health. 2021;6(7).

48. Afrane YA, Zhou G, Githeko AK, Yan G. Utility of health facility-based malaria data for malaria surveillance. PLoS One. 2013;8(2):e54305.

49. Yeka A, Gasasira A, Mpimbaza A, Achan J, Nankabirwa J, Nsobya S, et al. Malaria in Uganda: challenges to control on the long road to elimination: I. Epidemiology and current control efforts. Acta Trop. 2012;121(3):184-95.

50. Namuganga JF, Epstein A, Nankabirwa JI, Mpimbaza A, Kiggundu M, Sserwanga A, et al. The impact of stopping and starting indoor residual spraying on malaria burden in Uganda. Nat Commun. 2021;12(1):2635.

51. Kigozi SP, Kigozi RN, Sebuguzi CM, Cano J, Rutazaana D, Opigo J, et al. Spatial-temporal patterns of malaria incidence in Uganda using HMIS data from 2015 to 2019. BMC Public Health. 2020;20(1):1913.

52. World Health Organization. Framework for implementing the Global Technical Strategy for Malaria 2016–2030 in the African region. 2016.

53. Weiss DJ, Mappin B, Dalrymple U, Bhatt S, Cameron E, Hay SI, et al. Re-examining environmental correlates of Plasmodium falciparum malaria endemicity: a data-intensive variable selection approach. Malar J. 2015;14:68.

54. Funk C, Peterson P, Landsfeld M, Pedreros D, Verdin J, Shukla S, et al. The climate hazards infrared precipitation with stations--a new environmental record for monitoring extremes. Sci Data. 2015;2:150066.

55. Zhengming Wan - University of California Santa Barbara SH, Glynn Hulley - JPL and MODAPS SIPS - NASA;. MOD11C1 MODIS/Terra Land Surface Temperature and the Emissivity Daily L3 Global 0.05Deg CMG. NASA LP DAAC; 2015.

56. Kamel Didan - University of Arizona AH-UoTSaMS-N. MOD13Q1 MODIS/Terra Vegetation Indices 16-Day L3 Global 250m SIN Grid. NASA LP DAAC; 2015.

57. Jarvis A, Reuter H, Nelson A, Guevara E. Hole-filled SRTM for the globe Version 4, available from the CGIAR-CSI SRTM 90m. In: http://srtm.csi.cgiar.org, editor. 2008.

58. Ferranti Jd. 'Digital Elevation Data'. Viewfinder Panoramas (www.viewfinderPanoramas.org/dem3.html); based on NASA's Shuttle Radar Topography Mission (SRTM) data (http://www2.jpl.nasa.gov/srtm/). 2017.

59. WorldPop (www.worldpop.org - School of Geography and Environmental Science, University of Southampton, Department of Geography and Geosciences, University of

Louisville, Departement de Geographie, Universite de Namur) and Center for International Earth Science Information Network (CIESIN). Global High Resolution Population Denominators Project - Funded by The Bill and Melinda Gates Foundation (OPP1134076). 2018.

60. Tusting LS, Bisanzio D, Alabaster G, Cameron E, Cibulskis R, Davies M, et al. Mapping changes in housing in sub-Saharan Africa from 2000 to 2015. Nature. 2019.

61. Elvidge CD, Baugh K, Zhizhin M, Ghosh FCH. VIIRS night-time lights. International Journal of Remote Sensing. 2017;38(21):5860-79.

62. Epstein A, Namuganga JF, Kamya EV, Nankabirwa JI, Bhatt S, Rodriguez-Barraquer I, et al. Estimating malaria incidence from routine health facility-based surveillance data in Uganda. Malar J. 2020;19(1):445.

63. Tatem AJ. WorldPop, open data for spatial demography. Sci Data. 2017;4:170004.

64. Wood SN. Generalized Additive Models: An Introduction with R2017.

65. Rue H, Held L. Gaussian Markov Random Fields: Theory and Applications2005.

66. Sherrard-Smith E, Griffin JT, Winskill P, Corbel V, Pennetier C, Djenontin A, et al. Systematic review of indoor residual spray efficacy and effectiveness against Plasmodium falciparum in Africa. Nat Commun. 2018;9(1):4982.

67. Choi L, Pryce J, Garner P. Indoor residual spraying for preventing malaria in communities using insecticide-treated nets. Cochrane Database Syst Rev. 2019;5:CD012688.

68. WHO. Global Plan for Inescticide Resistance Management in Malaria Vectors. 2012.

69. Ministry of Health. The Uganda Malaria Reduction Strategic Plan 2014-2020. Kampala, Uganda; 2014.

70. Wagman J, Cisse I, Kone D, Fomba S, Eckert E, Mihigo J, et al. Rapid reduction of malaria transmission following the introduction of indoor residual spraying in previously

unsprayed districts: an observational analysis of Mopti Region, Mali, in 2017. Malar J. 2020;19(1):340.

71. Kane F, Keita M, Traore B, Diawara SI, Bane S, Diarra S, et al. Performance of IRS on malaria prevalence and incidence using pirimiphos-methyl in the context of pyrethroid resistance in Koulikoro region, Mali. Malar J. 2020;19(1):286.

72. Gogue C, Wagman J, Tynuv K, Saibu A, Yihdego Y, Malm K, et al. An observational analysis of the impact of indoor residual spraying in Northern, Upper East, and Upper West Regions of Ghana: 2014 through 2017. Malar J. 2020;19(1):242.

73. Hast MA, Chaponda M, Muleba M, Kabuya JB, Lupiya J, Kobayashi T, et al. The Impact of 3 Years of Targeted Indoor Residual Spraying With Pirimiphos-Methyl on Malaria Parasite Prevalence in a High-Transmission Area of Northern Zambia. Am J Epidemiol. 2019;188(12):2120-30.

74. Abong'o B, Gimnig JE, Torr SJ, Longman B, Omoke D, Muchoki M, et al. Impact of indoor residual spraying with pirimiphos-methyl (Actellic 300CS) on entomological indicators of transmission and malaria case burden in Migori County, western Kenya. Scientific reports. 2020;10(1):4518.

75. Tchouakui M, Mugenzi LMJ, B DM, Khaukha JNT, Tchapga W, Tchoupo M, et al. Pyrethroid Resistance Aggravation in Ugandan Malaria Vectors Is Reducing Bednet Efficacy. Pathogens. 2021;10(4).

76. Okia M, Hoel DF, Kirunda J, Rwakimari JB, Mpeka B, Ambayo D, et al. Insecticide resistance status of the malaria mosquitoes: Anopheles gambiae and Anopheles funestus in eastern and northern Uganda. Malar J. 2018;17(1):157.

77. Lynd A, Gonahasa S, Staedke SG, Oruni A, Maiteki-Sebuguzi C, Dorsey G, et al. LLIN Evaluation in Uganda Project (LLINEUP): a cross-sectional survey of species diversity and insecticide resistance in 48 districts of Uganda. Parasit Vectors. 2019;12(1):94.

78. Oxborough RM, Seyoum A, Yihdego Y, Dabire R, Gnanguenon V, Wat'senga F, et al. Susceptibility testing of Anopheles malaria vectors with the neonicotinoid insecticide clothianidin; results from 16 African countries, in preparation for indoor residual spraying with new insecticide formulations. Malar J. 2019;18(1):264.

79. Marti-Soler H, Maquina M, Opiyo M, Alafo C, Sherrard-Smith E, Malheia A, et al. Effect of wall type, delayed mortality and mosquito age on the residual efficacy of a clothianidin-based indoor residual spray formulation (SumiShield 50WG) in southern Mozambique. PLoS One. 2021;16(8):e0248604.

80. Agossa FR, Padonou GG, Koukpo CZ, Zola-Sahossi J, Azondekon R, Akuoko OK, et al. Efficacy of a novel mode of action of an indoor residual spraying product, SumiShield(R) 50WG against susceptible and resistant populations of Anopheles gambiae (s.l.) in Benin, West Africa. Parasit Vectors. 2018;11(1):293.

81. Ngwej LM, Hattingh I, Mlambo G, Mashat EM, Kashala JK, Malonga FK, et al. Indoor residual spray bio-efficacy and residual activity of a clothianidin-based formulation (SumiShield((R)) 50WG) provides long persistence on various wall surfaces for malaria control in the Democratic Republic of the Congo. Malar J. 2019;18(1):72.

82. Kweka E, Mahande A, Ouma J, Karanja W, Msangi S, Temba V, et al. Novel Indoor Residual Spray Insecticide With Extended Mortality Effect: A Case of SumiShield 50WG Against Wild Resistant Populations of Anopheles arabiensis in Northern Tanzania. Glob Health Sci Pract. 2018;6(4):758-65.

83. Fongnikin A, Houeto N, Agbevo A, Odjo A, Syme T, N'Guessan R, et al. Efficacy of Fludora(R) Fusion (a mixture of deltamethrin and clothianidin) for indoor residual spraying against pyrethroid-resistant malaria vectors: laboratory and experimental hut evaluation. Parasit Vectors. 2020;13(1):466.

84. Fuseini G, Phiri WP, von Fricken ME, Smith J, Garcia GA. Evaluation of the residual effectiveness of Fludora fusion WP-SB, a combination of clothianidin and deltamethrin, for the control of pyrethroid-resistant malaria vectors on Bioko Island, Equatorial Guinea. Acta Trop. 2019;196:42-7.

85. Agossa FR, Padonou GG, Fassinou A, Odjo EM, Akuoko OK, Salako A, et al. Small-scale field evaluation of the efficacy and residual effect of Fludora((R)) Fusion (mixture of clothianidin and deltamethrin) against susceptible and resistant Anopheles gambiae populations from Benin, West Africa. Malar J. 2018;17(1):484.

86. Seelig F, Bezerra H, Cameron M, Hii J, Hiscox A, Irish S, et al. The COVID-19 pandemic should not derail global vector control efforts. PLoS Negl Trop Dis. 2020;14(8):e0008606.

87. Guerra CA, Tresor Donfack O, Motobe Vaz L, Mba Nlang JA, Nze Nchama LO, Mba Eyono JN, et al. Malaria vector control in sub-Saharan Africa in the time of COVID-19: no room for complacency. BMJ Glob Health. 2020;5(9).

88. Lindsay SW, Thomas MB, Kleinschmidt I. Threats to the effectiveness of insecticide-treated bednets for malaria control: thinking beyond insecticide resistance. Lancet Glob Health. 2021;9(9):e1325-e31.

89. Mawejje HD, Kilama M, Kigozi SP, Musiime AK, Kamya M, Lines J, et al. Impact of seasonality and malaria control interventions on Anopheles density and species composition from three areas of Uganda with differing malaria endemicity. Malar J. 2021;20(1):138.

90. Staedke SG, Gonahasa S, Dorsey G, Kamya MR, Maiteki-Sebuguzi C, Lynd A, et al. Effect of long-lasting insecticidal nets with and without piperonyl butoxide on malaria indicators in Uganda (LLINEUP): a pragmatic, cluster-randomised trial embedded in a national LLIN distribution campaign. Lancet. 2020;395(10232):1292-303.

Publishing Agreement

It is the policy of the University to encourage open access and broad distribution of all theses, dissertations, and manuscripts. The Graduate Division will facilitate the distribution of UCSF theses, dissertations, and manuscripts to the UCSF Library for open access and distribution. UCSF will make such theses, dissertations, and manuscripts accessible to the public and will take reasonable steps to preserve these works in perpetuity.

I hereby grant the non-exclusive, perpetual right to The Regents of the University of California to reproduce, publicly display, distribute, preserve, and publish copies of my thesis, dissertation, or manuscript in any form or media, now existing or later derived, including access online for teaching, research, and public service purposes.

DocuSigned by:
97915BC9DB88474...
Author Signature

11/28/2021
Date